



Published in final edited form as:

Nature. 2023 August ; 620(7975): 881–889. doi:10.1038/s41586-023-06409-6.

## Lactate limits CNS autoimmunity by stabilizing HIF-1 $\alpha$ in dendritic cells

Liliana M. Sanmarco<sup>1</sup>, Joseph M. Rone<sup>1,2</sup>, Carolina M. Polonio<sup>1</sup>, Gonzalo Fernandez Lahore<sup>1,2</sup>, Federico Giovannoni<sup>1</sup>, Klynne Ferrara<sup>1</sup>, Cristina Gutierrez-Vazquez<sup>1</sup>, Ning Li<sup>3</sup>, Anna Sokolovska<sup>3</sup>, Agustin Plasencia<sup>1</sup>, Camilo Faust Aki<sup>1</sup>, Payal Nanda<sup>1</sup>, Evelin S. Heck<sup>1</sup>, Zhaorong Li<sup>1</sup>, Hong-Gyun Lee<sup>1</sup>, Chun-Cheih Chao<sup>1</sup>, Claudia M. Rejano-Gordillo<sup>1</sup>, Pedro H. Fonseca-Castro<sup>1</sup>, Tomer Illouz<sup>1</sup>, Mathias Linnerbauer<sup>1</sup>, Jessica E. Kenison<sup>1</sup>, Rocky M. Barilla<sup>1,2</sup>, Daniel Farrenkopf<sup>1</sup>, Nikolas A. Stevens<sup>1</sup>, Gavin Piester<sup>1</sup>, Elizabeth N. Chung<sup>1</sup>, Lucas Dailey<sup>4</sup>, Vijay K. Kuchroo<sup>1,2</sup>, David Hava<sup>3</sup>, Michael A. Wheeler<sup>1,4</sup>, Clary Clish<sup>4</sup>, Roni Nowarski<sup>1,2</sup>, Eduardo Balsa<sup>5</sup>, Jose M. Lora<sup>3</sup>, Francisco J. Quintana<sup>1,4</sup>

<sup>1</sup>Ann Romney Center for Neurologic Diseases, Harvard Medical School, Brigham and Women's Hospital, Boston, MA, USA.

<sup>2</sup>Evergrande Center for Immunologic Diseases, Harvard Medical School, Brigham and Women's Hospital, Boston, MA, USA.

<sup>3</sup>Synlogic Therapeutics, Cambridge, MA, USA.

<sup>4</sup>Broad Institute of MIT and Harvard, Cambridge, MA, USA.

<sup>5</sup>Centro de Biología Molecular Severo Ochoa UAM-CSIC, Universidad Autónoma de Madrid, Madrid, Spain.

### Abstract

Dendritic cells (DCs) have a role in the development and activation of self-reactive pathogenic T cells<sup>1,2</sup>. Genetic variants that are associated with the function of DCs have been linked to autoimmune disorders<sup>3,4</sup>, and DCs are therefore attractive the rapeutic targets for such

Reprints and permissions information is available at <http://www.nature.com/reprints>.

Correspondence and requests for materials should be addressed to Francisco J. Quintana. [fquintana@rics.bwh.harvard.edu](mailto:fquintana@rics.bwh.harvard.edu).  
**Author contributions** L.M.S., J.M.R., C.M.P., G.F.L., F.G., K.F., C.G.-V., N.L., A.S., A.P., C.F.A., P.N., E.S.H., H.-G.L., C.-C.C., C.M.R.-G., P.H.F.-C., M.L., J.E.K., R.M.B., D.F., G.P., E.N.C., N.A.S. and L.D. performed in vitro and in vivo experiments, FACS and genomic experiments. L.M.S., Z.L. and M.A.W. performed bioinformatic analyses. T.I. performed unbiased quantification of histology samples. J.M.R., C.C., V.K.K. and R.N. contributed reagents. L.M.S., N.L., D.H., A.S., J.M.L. and F.J.Q. designed and generated engineered probiotics. L.M.S., E.B. and F.J.Q. discussed and interpreted findings and wrote the manuscript with input from the other co-authors. F.J.Q. designed and supervised the study and edited the manuscript.

#### Online content

Any methods, additional references, Nature Portfolio reporting summaries, source data, extended data, supplementary information, acknowledgements, peer review information; details of author contributions and competing interests; and statements of data and code availability are available at <https://doi.org/10.1038/s41586-023-06409-6>.

**Competing interests** N.L., A.S., D.H. and J.M.L. were employees of Synlogic Therapeutics during some of this study. The remaining authors declare no competing interests.

#### Additional information

**Supplementary information** The online version contains supplementary material available at <https://doi.org/10.1038/s41586-023-06409-6>.

**Peer review information** Nature thanks Greg Delgoffe, Lawrence Steinman and the other, anonymous, reviewer(s) for their contribution to the peer review of this work.

diseases. However, developing DC-targeted therapies for autoimmunity requires identification of the mechanisms that regulate DC function. Here, using single-cell and bulk transcriptional and metabolic analyses in combination with cell-specific gene perturbation studies, we identify a regulatory loop of negative feedback that operates in DCs to limit immunopathology. Specifically, we find that lactate, produced by activated DCs and other immune cells, boosts the expression of NDUFA4L2 through a mechanism mediated by hypoxia-inducible factor 1 $\alpha$  (HIF-1 $\alpha$ ). NDUFA4L2 limits the production of mitochondrial reactive oxygen species that activate XBP1-driven transcriptional modules in DCs that are involved in the control of pathogenic autoimmune T cells. We also engineer a probiotic that produces lactate and suppresses T cell autoimmunity through the activation of HIF-1 $\alpha$ –NDUFA4L2 signalling in DCs. In summary, we identify an immunometabolic pathway that regulates DC function, and develop a synthetic probiotic for its therapeutic activation.

---

DCs are professional antigen-presenting cells with central roles in the control of adaptive immunity<sup>1,2</sup>. In the context of autoimmune diseases, DCs regulate tissue pathology through a variety of mechanisms, including the priming and differentiation of pathogenic and regulatory T cells, the local reactivation of autoimmune T cells in target tissues and the control of epitope spreading<sup>1,2</sup>. Genetic variants associated with DC function have been linked to autoimmune disorders<sup>3,4</sup>, highlighting the importance of DCs in immune regulation. On the basis of these findings, DCs are seen as attractive therapeutic targets for the management of human autoimmune diseases. However, designing successful therapies for autoimmunity requires the identification of the regulatory mechanisms that control DC responses. Some key mechanisms linked to the regulation of DCs in cancer have been described<sup>5,6</sup>, but less is known about how these cells are regulated in the context of autoimmunity.

Metabolism regulates adaptive and innate immunity, with major implications for the pathology of autoimmune diseases<sup>7</sup>. In addition, metabolites produced by hosts<sup>8</sup> and by commensal flora<sup>9</sup> can regulate the function of DCs, which suggests that approaches based on probiotics could allow the therapeutic modulation of DC responses in autoimmune diseases. However, unmanipulated probiotics use built-in anti-inflammatory mechanisms that are evolutionarily selected to optimize interactions between the host and the commensal microorganisms in health, but not in the context of autoimmune pathology<sup>10</sup>. Moreover, the mechanism of action of unmanipulated probiotics is often unclear, which limits their utility for mechanistic studies. For example, *Lactobacillus reuteri* is frequently used as a source of anti-inflammatory agonists for the aryl hydrocarbon receptor (AHR), but its therapeutic effects on neurological disorders involve additional metabolites acting through AHR-independent pathways<sup>11</sup>. Synthetic biology allows the design of probiotics that are optimized for immune modulation through well-defined mechanisms of action, as exemplified in reports of engineered probiotics targeting L-arginine<sup>12</sup> and purinergic signalling<sup>13</sup> in the context of cancer immunotherapy and inflammatory bowel disease, respectively.

In this study, we combined single-cell and bulk transcriptional and metabolic analyses with gene perturbation studies to investigate the regulation of DCs in autoimmunity.

We found that L-LA upregulates the expression of NDUFA4L2 (NADH dehydrogenase (ubiquinone)-1 $\alpha$  subcomplex 4-like 2) through a mechanism mediated by the transcription factor HIF-1 $\alpha$ . NDUFA4L2 controls mitochondrial activity in DCs, limiting the expression of mitochondrial reactive oxygen species (mtROS)-driven transcriptional programs that promote the differentiation of encephalitogenic T cells. Moreover, we developed a synthetic probiotic engineered to produce lactate, which limits T-cell-driven central nervous system (CNS) autoimmunity in experimental autoimmune encephalomyelitis (EAE) through the activation of HIF-1 $\alpha$ -NDU-FA4L2 signalling in DCs. In summary, we identify a immunometabolic pathway that limits DC pro-inflammatory responses, and we engineer synthetic probiotics with which to modulate this pathway in therapies for autoimmune disorders.

## HIF-1 $\alpha$ expression in DCs limits T cell autoimmunity

To identify mechanisms involved in the regulation of DCs in CNS autoimmunity, we used single-cell RNA sequencing (scRNA-seq) to analyse DCs recruited to the CNS in EAE induced in B6 mice by immunization with MOG<sub>35–55</sub>. We detected the activation of transcriptional programs associated with inflammation, such as NF- $\kappa$ B, PI3K-AKT and TLR signalling (Fig. 1a). We also observed the activation of signalling by the transcription factor HIF-1 $\alpha$  in both type 1 and type 2 classic DCs (cDC1s and cDC2s), in which HIF-1 $\alpha$  protein was also expressed (Fig. 1a,b and Extended Data Fig. 1a–d). Accordingly, we detected an upregulation of the levels of HIF-1 $\alpha$  protein in DCs in the CNS, lymph nodes and spleen at the onset of EAE (Fig. 1c,d).

HIF-1 $\alpha$ -driven transcriptional responses have been studied in the context of tumour immune evasion<sup>14</sup>, but much less is known about the control of DCs by HIF-1 $\alpha$  during autoimmunity. To study the role of HIF-1 $\alpha$  in DCs during CNS inflammation we generated *Itgax<sup>Cre</sup> Hif1a<sup>flox</sup>* (HIF-1 $\alpha$ <sup>Itgax</sup>) mice. Deletion of the gene encoding HIF-1 $\alpha$  in DCs resulted in a worsening of EAE, concomitant with increased numbers of IFN $\gamma$ <sup>+</sup>, IL-17<sup>+</sup> and GM-CSF<sup>+</sup> CD4<sup>+</sup> T cells in the CNS and the periphery, and increased recall responses to MOG<sub>35–55</sub> (Fig. 1e,f and Extended Data Fig. 1e–g). The recruitment of DCs to the CNS was unaffected (Extended Data Fig. 1i).

RNA-seq analyses of HIF-1 $\alpha$ -deficient splenic DCs detected an increased activation of pathways linked to inflammation and abnormal mitochondrial respiratory function during EAE (Fig. 1g–i). Similarly, HIF-1 $\alpha$ -deficient DCs that were isolated from the CNS during EAE showed increased transcriptional responses linked to neuroinflammation, the production of reactive oxygen species (ROS) and the response to mitochondrial depolarization (gene set enrichment analysis (GSEA) gene ontology (GO) pathway 0098780; Extended Data Fig. 1j–l and Table 1).

To validate these findings, we analysed the response of bone-marrow-derived DCs (BMDCs) to hypoxia (1% oxygen) and other stimuli that stabilize HIF-1 $\alpha$  and increase its intracellular levels, such as deferoxamine, ML228 and the knockdown of the Von Hippel–Lindau tumour suppressor (VHL). Stabilization of HIF-1 $\alpha$  decreased the expression of *Il1b*, *Il6*, *Il23a*, *Tnf* and *Il12a* in DCs (Extended Data Fig. 2a–c) and the expression of *Ifng* and *Il17a* in

co-cultured 2D2<sup>+</sup>CD4<sup>+</sup> T cells in the presence of their cognate antigen MOG<sub>35–55</sub> (Extended Data Fig. 2d). HIF-1 $\alpha$  stabilization did not affect the viability of DCs (Extended Data Fig. 2e,f).

To further investigate the role of HIF-1 $\alpha$  in the control of the T cell response, we infected HIF-1 $\alpha$ <sup>Igax</sup> mice with *Salmonella enterica* subsp. *enterica* serovar Typhimurium (*S. typhimurium*) expressing the T cell epitope 2W1S (ref. 15) (Extended Data Fig. 2g). Loss of HIF-1 $\alpha$  in DCs resulted in a lower caecal bacteria burden and a concomitant increase in 2WS1-specific CD4<sup>+</sup> T cells, and IFN $\gamma$ <sup>+</sup>CD4<sup>+</sup> and IL-17<sup>+</sup>CD4<sup>+</sup> T cells, in the colon (Extended Data Fig. 2h–j). Together, these findings suggest that HIF-1 $\alpha$  limits DC transcriptional programs that promote effector T cell responses.

## Activation of HIF-1 $\alpha$ by lactate inhibits DC responses

Metabolites can stabilize HIF-1 $\alpha$  (ref. 16). We thus evaluated the effect of metabolites on the intracellular levels of HIF-1 $\alpha$  in splenic DCs. L-lactate (L-LA) induced the highest expression of HIF-1 $\alpha$  (Fig. 1j,k and Extended Data Fig. 3a,b), and activated HIF-1 $\alpha$ -driven gene expression in BMDCs from ODD-Luc mice, which contain a HIF-1 $\alpha$ -responsive luciferase reporter<sup>17</sup> (Extended Data Fig. 3c). Notably, lipopolysaccharide (LPS) increased the production of L-LA, the expression of *Hif1a* and the protein levels of HIF-1 $\alpha$  in DCs (Fig. 1k and Extended Data Fig. 3d,e), suggesting that DC activation induces both *Hif1a* expression and lactate-dependent stabilization of HIF-1 $\alpha$ .

Treatment with L-LA decreased the LPS-induced expression of pro-inflammatory cytokines in primary mouse and human DCs (Fig. 1l and Extended Data Fig. 3f,g). In addition, pre-treating DCs with L-LA decreased the expression of *Ifng*, *Il17a* and *Csf2* in 2D2<sup>+</sup>CD4<sup>+</sup> T cells co-cultured in the presence of MOG<sub>35–55</sub> (Fig. 1m). These anti-inflammatory effects of L-LA were dose-dependent and involved monocarboxylate transporter 1 (MCT1)—which transports L-LA across the cell membrane<sup>18</sup>—but not the GPR81 membrane receptor<sup>19</sup> (Fig. 1l and Extended Data Fig. 3h–j). Moreover, the anti-inflammatory effects of L-LA were HIF-1 $\alpha$ -dependent in mice and human DCs (Fig. 1n and Extended Data Figs. 3g and 4a–c). These findings suggest that the activation of DCs triggers an anti-inflammatory feedback loop driven by L-LA and HIF-1 $\alpha$ .

Two lactate stereoisomers exist in nature: L-LA is produced by mammalian cells, whereas d-lactate (D-LA) is provided by the diet, the microbiome and the methylglyoxal pathway<sup>20</sup>. D-LA and L-LA both induced the upregulation of HIF-1 $\alpha$  protein in mouse DCs (Fig. 1k and Extended Data Fig. 4d). Moreover, D-LA recapitulated the anti-inflammatory activities of L-LA, decreasing the expression of pro-inflammatory cytokines in mouse and human DCs and reducing the polarization of effector T cells in co-culture studies (Fig. 1n and Extended Data Figs. 3g and 4e,f). Thus, the activation of HIF-1 $\alpha$  by L-LA or D-LA limits pro-inflammatory DC responses.

## HIF-1 $\alpha$ -induced NDUFA4L2 limits mtROS production

HIF-1 $\alpha$  controls several biological processes, including metabolism<sup>21</sup>. In line with this, HIF-1 $\alpha$ -deficient DCs showed decreases in glucose-transporter expression and in glycolytic

activity (Extended Data Fig. 5a–c). Moreover, HIF-1 $\alpha$  deficiency resulted in an increased oxygen consumption rate (OCR), and L-LA decreased the OCR in wild-type but not in HIF-1 $\alpha$ <sup>I $\alpha$ gax</sup> DCs (Fig. 2a). Of note, the levels of ATP in DCs were decreased by treatment with L-LA (Fig. 2b). Because we detected transcriptional modules that are linked to abnormal activity of the mitochondrial respiratory chain in HIF-1 $\alpha$ <sup>I $\alpha$ gax</sup> DCs (Fig. 1i), and because of the HIF-1 $\alpha$ -dependent effects of L-LA on the OCR (Fig. 2a), we analysed the expression of mitochondrial HIF-1 $\alpha$  target genes in BMDCs. We found a HIF-1 $\alpha$ -dependent increase in the expression of *Ndufa412* after stimulating DCs with LPS or treating them with L-LA or D-LA (Fig. 2c–e). Moreover, treatment with LPS, L-LA or D-LA increased *Ndufa412* expression, and overexpression of HIF-1 $\alpha$  transactivated the *Ndufa412* promoter, in reporter assays (Fig. 2e,f and Extended Data Fig. 5d).

NDUFA4L2 is a subunit of respiratory complex I that limits the activity of this complex and the generation of mitochondrial reactive oxygen species (mtROS)<sup>22</sup>. Overexpression of *Ndufa412* abolished the increase in basal respiration and proton leakage that was induced by HIF-1 $\alpha$  deletion, suggesting that HIF-1 $\alpha$ -driven expression of *Ndufa412* restricts mitochondrial respiration in DCs (Extended Data Fig. 5e,f). Moreover, overexpression of *Ndufa412* limited the expression of pro-inflammatory cytokines in DCs (Fig. 2g).

Complex I produces pro-inflammatory mtROS as a by-product<sup>23</sup>. L-LA and D-LA limited mtROS production and oxygen consumption in DCs in an *Ndufa412*-dependent manner, because knockdown of *Ndufa412* suppressed the effects of L-LA on the OCR and on mtROS production (Fig. 2h–j and Extended Data Fig. 5f). *Ndufa412* knockdown also abolished the anti-inflammatory effects of L-LA and D-LA on DCs (Fig. 2k and Extended Data Fig. 5g).

To investigate the link between lactate, mtROS and DC responses, we used mitoParaquant (mitoPQ), which selectively increases the production of mtROS, and the mtROS scavenger mitoTempo. MitoPQ boosted the LPS-induced expression of pro-inflammatory genes in DCs, whereas mitoTempo suppressed it (Fig. 2l). Moreover, mitoPQ abolished the inhibitory effects of L-LA on the expression of pro-inflammatory cytokines by DCs (Extended Data Fig. 6a,b), suggesting that the NDU-FA4L2-dependent suppression of mtROS production mediates the anti-inflammatory effects of lactate in DCs.

L-LA can be converted to pyruvate to enter the tricarboxylic acid (TCA) cycle<sup>24</sup>. However, using uniformly labelled <sup>13</sup>C-lactate, we detected very low levels of label incorporation (about 1%) into TCA intermediates in BMDCs (Extended Data Fig. 6c). In addition, treatment with L-LA or D-LA did not increase the intracellular levels of pyruvate (Extended Data Fig. 6d), and inhibiting the oxidation of L-LA into pyruvate by oxamate did not abolish the tolerogenic effects of lactate on DCs (Extended Data Fig. 6e,f), overall suggesting that the conversion of lactate into pyruvate and its use as a fuel does not contribute to lactate's anti-inflammatory effects in DCs. Indeed, pyruvate did not suppress pro-inflammatory gene expression in DCs (Extended Data Fig. 6g). Together, these data suggest that, by limiting the activity of complex I, the lactate- and HIF-1 $\alpha$ -driven expression of NDUFA4L2 limits mtROS-induced pro-inflammatory responses in DCs.

## L-LA limits mtROS-driven XBP1 activation in DCs

ROS<sup>23</sup> and inflammation<sup>25</sup> activate the unfolded protein response and the transcription factor XBP1, which drives pro-inflammatory responses in DCs<sup>23</sup> and macrophages<sup>25</sup>. Specifically, ROS and inflammation trigger the excision of an intron from the *Xbp1* mRNA, generating a spliced *Xbp1* mRNA (sXbp1), which encodes a full-length functional XBP1. L-LA reduced the activation of XBP1 in mouse BMDCs and human DCs, as indicated by an analysis of *Xbp1* mRNA splicing, but this effect was lost when mtROS generation was induced with mitoPQ (Fig. 3a,b and Extended Data Fig. 7a,b). Moreover, L-LA reduced the recruitment of XBP1 to the *Il1b*, *Il6* and *Il23a* promoters triggered by LPS (Fig. 3c–e). Conversely, mtROS production triggered by mitoPQ boosted the LPS-induced recruitment of XBP1 to pro-inflammatory cytokine promoters (Extended Data Fig. 7c).

In support of the hypothesis that HIF-1 $\alpha$  has a role in limiting XBP1 activation, we detected increased *Xbp1* mRNA splicing in HIF-1 $\alpha$ -deficient splenic DCs during EAE (Fig. 3f), and reduced recruitment of XBP1 to pro-inflammatory cytokine promoters after stabilization of HIF-1 $\alpha$  with ML228 (Extended Data Fig. 7d). Similarly, overexpression of *Ndufa4l2* reduced the LPS-induced splicing of *Xbp1* mRNA (Fig. 3g), suggesting that *Ndufa4l2* expression driven by HIF-1 $\alpha$  limits the activation of XBP1.

We also induced EAE in *Itgax<sup>Cre</sup>Xbp1<sup>flox</sup>* (*Xbp1<sup>Itgax</sup>*) mice<sup>26</sup>. EAE was ameliorated in *Xbp1<sup>Itgax</sup>* mice, concomitant with a reduction in IFN $\gamma$ <sup>+</sup>, IL-17<sup>+</sup> and IFN $\gamma$ <sup>+</sup>IL-17<sup>+</sup> CD4<sup>+</sup> T cells in the spleen and the CNS, and a decreased recall response to MOG<sub>35–55</sub> (Fig. 3h–k and Extended Data Fig. 7e). In RNA-seq analyses, XBP1-deficient DCs exhibited a decreased pro-inflammatory response (Fig. 4l,m and Extended Data Fig. 7f,g). Collectively, these findings suggest that, by limiting the production of mtROS, L-LA- and HIF-1 $\alpha$ -driven *Ndufa4l2* expression suppresses XBP1-dependent pro-inflammatory responses in DCs.

## Engineered probiotics activate HIF-1 $\alpha$ –NDUFA4L2

Finally, we studied the therapeutic potential of activating HIF-1 $\alpha$ –NDUFA4L2 signalling. Administration of L-LA or D-LA (125 mg per kg body weight, daily) suppressed the development of encephalitogenic T cells and EAE induced by MOG<sub>35–55</sub> immunization (Extended Data Fig. 8a,b) and limited the expression of genes linked to inflammation, mitochondrial metabolism, oxidative stress and the unfolded protein response in DCs (Extended Data Fig. 8c–f). Of note, the plasma levels of D-LA and L-LA were similar in EAE and in naive mice (Extended Data Fig. 9a).

To facilitate the intestinal absorption of lactate after oral delivery, while minimizing the potential for lactic acidosis associated with bolus lactate administration<sup>20</sup>, we engineered probiotics that produce D-LA (EcN<sup>Lac</sup>) (Fig. 4a). Specifically, we knocked out the *pta* gene in *Escherichia coli* Nissle (EcN), which has already been used to develop probiotics that have been tested in humans<sup>12,27,28</sup>, and introduced a plasmid containing the *ldhA* gene under the control of a heat-inducible promoter active at 37 °C, to ensure sufficient conversion of pyruvate to D-LA (refs. 29,30) (Fig. 4a and Extended Data Fig. 9b,c). Sequencing of the bacterial chromosome confirmed the deletion of *pta* (Extended Data Fig. 9b).

We first evaluated the ability of the heat-inducible promoter to drive the expression of GFP in an EcN strain (EcN<sup>GFP</sup>), and detected GFP expression 20 min after heat activation at 37 °C (Extended Data Fig. 9d,e). Similarly, the EcN<sup>Lac</sup> strain, but not the parental EcN strain, secreted D-LA when cultured at 37 °C (Fig. 4b); we did not detect any production of L-LA by EcN<sup>Lac</sup> (Fig. 4b).

To characterize the distribution and biological effects of probiotic-produced D-LA, we administered EcN<sup>Lac</sup> or EcN to mice by oral gavage daily for a week, and quantified the levels of D-LA in the plasma, small intestine and colon 1 h, 4 h and 24 h after the last administration of the probiotic. Administration of EcN<sup>Lac</sup> increased the levels of D-LA in the plasma, and also in small intestine and colon tissue, but not in the cerebrospinal fluid (CSF) or in CNS lysates (Fig. 4c and Extended Data Fig. 9f–h). Moreover, EcN<sup>Lac</sup> gavage increased the protein levels of HIF-1 $\alpha$  and NDUFA4L2, and increased HIF-1 $\alpha$  signalling in small-intestinal DCs, whereas it decreased the expression of active XBP1 protein (Fig. 4d,e and Extended Data Fig. 9i–k). Of note, neither EcN<sup>Lac</sup> nor EcN<sup>GFP</sup> was detected in the bloodstream after oral gavage (Extended Data Fig. 9l,m). Together, these findings suggest that the local increase in D-LA that results from EcN<sup>Lac</sup> administration activates HIF-1 $\alpha$ –NDUFA4L2 signalling in intestinal DCs.

To evaluate the effects of HIF-1 $\alpha$ –NDUFA4L2 activation on CNS inflammation, we administered EcN<sup>Lac</sup> or EcN daily or weekly by gavage starting three days before the induction of EAE (Extended Data Fig. 9n). Administration of EcN<sup>Lac</sup> ameliorated EAE, decreasing the number of pro-inflammatory T cells in the CNS, small intestine and periphery and the recall response to MOG<sub>35–55</sub> (Fig. 4f–h and Extended Data Fig. 10a–g). However, EcN<sup>Lac</sup> did not affect the bacterial burden or the number of pathogen-specific CD4<sup>+</sup> T cells after challenge with *S. typhimurium* (Extended Data Fig. 10h–k).

The intestinal microbiome regulates pathogenic T cells in EAE<sup>31</sup>. Studies have shown that encephalitogenic T cells are primed in intestinal tissues, and then migrate to the spleen and CNS during EAE<sup>32,33</sup>. Thus, we analysed the effects of EcN<sup>Lac</sup> administration on intestinal DCs and T cells. EcN<sup>Lac</sup> increased the intracellular levels of HIF-1 $\alpha$  in DCs but not in neutrophils, monocytes or T cells in the small intestine (Fig. 4d,e and Extended Data Fig. 10l,m). Indeed, the reduction of pathogenic T cell responses and the amelioration of EAE by EcN<sup>Lac</sup> were abolished in HIF-1 $\alpha$ <sup>Itgax</sup> mice, suggesting that HIF-1 $\alpha$ , expressed in DCs, has a role in the anti-inflammatory effects of EcN<sup>Lac</sup> (Fig. 4f,g and Extended Data Fig. 10a). In agreement with this interpretation, intestinal DCs from EcN<sup>Lac</sup>-treated mice showed reduced *Xbp1* mRNA splicing and decreased expression of pro-inflammatory cytokines (Fig. 4i,j). Moreover, we detected a reduction in IFN $\gamma$ <sup>+</sup>CD4<sup>+</sup> and IL-17<sup>+</sup>CD4<sup>+</sup> T cells that migrated from the intestine to the spleen, as determined by the use of *CAG<sup>Kaede</sup>* mice expressing a photoconvertible fluorescent protein<sup>34</sup> (Fig. 4k,l); the total number of CD4<sup>+</sup> T cells migrating from the intestine to the spleen remained unaffected (Fig. 4l). These findings suggest that EcN<sup>Lac</sup> suppresses inflammation in the CNS through the D-LA-driven activation of HIF-1 $\alpha$ –NDUFA4L2 in intestinal DCs—and, potentially, in other cell types.

## Discussion

HIF-1 $\alpha$  has been reported to have immunosuppressive roles in the tumour microenvironment, but less is known about its role in autoimmunity. Hypoxia is considered the bona-fide HIF-1 $\alpha$  activator<sup>21</sup>, but metabolites such as succinate<sup>16</sup> can also activate HIF-1 $\alpha$ . Here we report that lactate-triggered activation of HIF-1 $\alpha$  induces the expression of NDUFA4L2, which limits mtROS- and XBP1-driven pro-inflammatory responses in DCs. Stimulating DCs with LPS or other microbial molecules promotes NF- $\kappa$ B-driven *Hif1a* expression<sup>35</sup>, which increases the levels of HIF-1 $\alpha$  available for stabilization by lactate, and consequently limits, through NDUFA4L2, the activation of pro-inflammatory responses by mtROS and XBP in DCs. Together with previous reports<sup>36</sup>, our findings suggest that an L-LA–HIF-1 $\alpha$ –NDUFA4L2 signalling axis participates in a negative feedback loop that limits the responses of DCs to minimize immunopathology, as described for IL-10 (ref. 37) and IL-27 (ref. 38). This pathway might also respond to nutrients, such as glucose, in the DC microenvironment<sup>39</sup>.

Lactate<sup>40</sup> and HIF-1 $\alpha$  (ref. 41) have been linked to epigenetic and metabolic regulatory mechanisms that operate in monocytes and macrophages. In addition, lactate can boost the immunosuppressive activity of macrophages<sup>14,40</sup> and FOXP3<sup>+</sup> regulatory T cells<sup>42</sup>. Hence, other mechanisms as well as the activation of HIF-1 $\alpha$ –NDUFA4L2 signalling in DCs could contribute to the suppression of EAE by EcN<sup>Lac</sup>. Indeed, the increased response to *S. typhimurium* infection in HIF-1 $\alpha$ <sup>Igax</sup> mice suggests a general immune activation, which might obscure the contribution of cell types other than DCs to the suppressive effects of EcN<sup>Lac</sup> on EAE.

The diet and the commensal microbiota are physiological sources of D-LA, and could therefore activate HIF-1 $\alpha$  in DCs and other cells in intestinal tissues as part of homeostatic anti-inflammatory mechanisms—resembling previous observations<sup>43,44</sup> made for AHR. Notably, both HIF-1 $\alpha$  (ref. 14) and AHR (ref. 45,46) are hyperactivated as part of tumour immunoevasion strategies, and HIF-1 $\alpha$  and AHR transcriptional activity requires dimerization with the same cofactor, HIF-1 $\beta$  (ARNT)<sup>47</sup>. These findings suggest a cross-talk between HIF-1 $\alpha$  and AHR signalling in DCs, as previously described in T cells<sup>48</sup>. Nevertheless, considering the paradoxical immunosuppressive effects of chronic XBP1 activation in the tumour microenvironment<sup>26</sup>, future studies should investigate the effects of chronic HIF-1 $\alpha$ –NDUFA4L2 signalling on XBP1-driven transcriptional programs.

In summary, we have identified a lactate-driven HIF-1 $\alpha$ –NDUFA4L2 signalling axis that operates in DCs to limit XBP1-driven transcriptional modules that promote T cell autoimmunity. Our study also suggests that HIF-1 $\alpha$ –NDUFA4L2 signalling could be a target for therapeutic intervention. Several immunomodulatory DC-targeting approaches have already been developed, including nanoliposomes engineered to co-deliver autoantigen and a tolerogenic AHR agonist<sup>49</sup>, or to deliver an autoantigen-encoding modified mRNA<sup>50</sup>. Engineered probiotics provide an alternative approach for therapeutic immunomodulation, enabling the administration of therapeutic agents on a long-term basis with minimal adverse effects. Indeed, the established safety profile, high serum sensitivity, broad antibiotic susceptibility, defined genomic landscape and high engineerability of EcN probiotics

support their use for the therapeutic activation of HIF-1 $\alpha$ -NDUFA4L2 signalling in autoimmunity. Probiotics engineered to activate immunoregulatory signalling pathways could provide new tools for the clinical management of autoimmune and allergic disorders.

## Methods

### Mice

Adult female mice were used on a C57Bl/6J background (The Jackson Laboratory, 000664), except for HIF-1 $\alpha$  reporter *FVB.129S6-Gt(ROSA)26Sortm2(HIF1A/luc)Kael/J* mice (The Jackson Laboratory, 006206). *B6.Cg-Tg(Itgax-cre)1-1Reiz/J* mice (The Jackson Laboratory, 008068) were bred with *B6.129-Hif1a<sup>tm3Rsj</sup>/J* mice (The Jackson Laboratory, 007561) to generate *Itgax<sup>Cre</sup>HIF-1 $\alpha$ <sup>fl</sup>* mice. *Itgax<sup>Cre</sup>XBP1<sup>fl</sup>* mice<sup>26</sup> were a gift from J. R. Cubillos Ruiz and L. Glimcher. *C57BL/6-Tg(Tcra2D2, Tcrb2D2)1Kuch/J* mice<sup>51</sup> (The Jackson Laboratory, 006912) were used for co-co-culture with DCs. All mice were housed in sterile autoclaved cages with irradiated food and acidified, autoclaved water. Mouse handling and weekly cage changes were performed by staff wearing sterile gowns, masks and gloves in a sterile biosafety hood. All mice were kept in a specific-pathogen-free facility at the Hale Building of Transformative Medicine at the Brigham and Women's Hospital. All mice were 8–10 weeks old at the time of EAE induction. All procedures were reviewed and approved under the guidelines of the Institutional Animal Care and Use Committee (IACUC) at Brigham and Women's Hospital.

### EAE

EAE was induced as described<sup>52,53</sup>, using 150  $\mu$ g of MOG<sub>35–55</sub> (Genemed Synthesis, 110582) mixed with complete Freund's adjuvant (20 ml incomplete Freund's adjuvant (BD Biosciences, BD263910) mixed with 100 mg *Mycobacterium tuberculosis* H-37Ra (BD Biosciences, 231141)) at a ratio of 1:1 (v/v at a concentration of 5 mg ml<sup>-1</sup>). All mice received two subcutaneous injections of 100  $\mu$ l each of the mix of MOG and complete Freund's adjuvant. All mice then received an intraperitoneal injection of *Pertussis* toxin (List Biological Laboratories, 180) at a concentration of 2 ng  $\mu$ l<sup>-1</sup> in 200  $\mu$ l phosphate-buffered saline (PBS) on the day of EAE induction and two days later. Mice were monitored daily and scored as follows: 0, no signs; 1, fully limp tail; 2, hindlimb weakness; 3, hindlimb paralysis; 4, forelimb paralysis; 5, moribund. Mice were randomly assigned to treatment groups. All mice were scored blind to genotype.

### Isolation of mouse CNS cells

CNS cells were isolated by flow cytometry as described<sup>52,53</sup>. In brief, mice were perfused with 1 $\times$  PBS, and the CNS was isolated, finely minced, digested in 0.66 mg ml<sup>-1</sup> papain (Sigma-Aldrich, P4762) in Hanks' balanced salt solution (HBSS) for 20 min and then incubated for 20 min with an equal volume of Dulbecco's modified Eagle's medium (DMEM) with collagenase D (Roche, 11088858001) and DNase I (Thermo Fisher Scientific, 90083) at 0.66 mg ml<sup>-1</sup> and 8 U ml<sup>-1</sup>, respectively. Samples were shaken at 80 rpm at 37 °C. Tissue was mechanically dissociated using a 5-ml serological pipette and filtered through a 70- $\mu$ m cell strainer (Fisher Scientific, 22363548) into a 50-ml conical. Tissue was centrifuged at 500g for 5 min and resuspended in 10 ml of 30% Percoll solution

(9 ml Percoll (GE Healthcare Biosciences, 17-5445-01), 3 ml 10× PBS, 18 ml ddH<sub>2</sub>O). The Percoll suspension was centrifuged at 500g for 25 min with no brakes. Supernatant was discarded and the cell pellet was washed with 1× PBS, centrifuged at 500g for 5 min and prepared for downstream applications.

### Isolation of mouse splenic cells

Spleens were incubated for 20 min with 2 mg ml<sup>-1</sup> collagenase D (Roche, 11088858001) and then mashed through a 70-µm cell strainer. Red blood cells were lysed with ACK lysing buffer (Life Technologies, A10492-01) for 5 min, and then washed with 0.5% BSA, 2 mM EDTA pH 8.0 in 1× PBS.

### Salmonella culturing and infection

A modified *S. Typhimurium* LVS strain BRD509 expressing a short peptide sequence recognizable by 2SW1 tetramer staining (provided by S. McSorley) was used for all experiments. A stab of bacterial glycerol stock was first cultured overnight in 3 ml Luria-Bertani (LB) broth at 37 °C in a shaking incubator at 200 rpm. The next day, a subculture was prepared using 30 µl of the original culture in 3 ml LB broth at 37 °C and 200 rpm for 4 h or until the optical density at 600 nm (OD<sub>600 nm</sub>) was in logarithmic range (0.6–0.9). The concentration of colony-forming units (CFU) was calculated using the conversion factor 1.0 (OD<sub>600 nm</sub>) = 1 × 10<sup>9</sup> CFU per ml. For infections, the bacteria culture was directly diluted to 1.25 × 10<sup>7</sup> CFU per ml in sterile PBS and 200 µl was injected through the tail vein. Doses were validated by serial dilution and plating on LB agar plates at 37 °C then counting the CFU 12 h later. Fourteen days after infection, the liver and caecum were weighted, then small pieces were weighed and used for CFU analysis. Tissue pieces were homogenized in 1 ml sterile PBS using the gentleMACS Dissociator (Miltenyi Biotec), then homogenates were serially diluted and plated in triplicate on LB agar plates incubated overnight at 37 °C. CFU counts were calculated per mg tissue, then extrapolated to total tissue burden using total tissue weights.

### Isolation of colon-infiltrating cells

In brief, tissue was cleaned, cut into 1-cm pieces and incubated with 20 ml of pre-warmed PBS containing 1 mM DTT (Thermo Fisher Scientific, P2325), 2.5 mM EDTA and 2.5% fetal bovine serum (FBS) for 20 min at 37 °C. Then, samples were rinsed with PBS and 20 ml of PBS containing 5 mM EDTA and 5% FBS was added for 20 min at 37 °C. Samples were rinsed three times with PBS on a nylon strainer, minced with scissors and digested with 1 mg ml<sup>-1</sup> collagenase VIII (Sigma-Aldrich, C2139-5G) and 40 U DNase (Thermo Fisher Scientific, 90083) in complete RPMI for 40 min at 37 °C. Finally, samples were filtered on 100-µm and 40-µm cell strainers and stained as described above. CD45<sup>+</sup> cells were isolated using a CD45 magnetic beads isolation kit (130-052-301, Miltenyi Biotec).

### Isolation of liver immune cells

Hepatic immune cells were isolated as described<sup>54</sup>. In brief, livers were obtained in PBS (Gibco) and passed through 100-mm nylon meshes; erythrocytes were removed using ACL

lysis buffer. Hepatocytes were separated from immune cells by a 35% and 70% bilayer Percoll gradient (GE Healthcare).

### Flow cytometry for S2W1 T cells

Cells were restimulated in RPMI containing 10% FBS (Gibco), 500 ng ml<sup>-1</sup> ionomycin (Sigma-Aldrich), 500 ng ml<sup>-1</sup> phorbol 12-myristate 13-acetate (PMA; Sigma-Aldrich), GolgiPlug and BD GolgiStop (BD Bioscience), and were incubated at 37 °C and 5% CO<sub>2</sub> for 4 h. Restimulated cells were then washed with PBS, and incubated for 30 min with dasatanib (5 nM, Sigma-Aldrich) and purified Fc block (553142, BD Biosciences), followed by a one-hour incubation with APC-labelled S2W1 tetramer (TS-M722-2, MBL International). Tetramer-stained cells were washed and stained using the following antibodies: BUV661-labelled anti-CD45 antibody (612975, BD Biosciences), BV650-labelled anti-CD3 antibody (740530, BD Biosciences) and PE-Cy7-labelled anti-CD4 antibody (100422, 100547, BioLegend). Cells were then fixed and permeabilized using the Foxp3 Fixation/Permeabilization kit (eBioscience). Intracellular antibodies were APC/Cy7 anti-mouse IFN $\gamma$  (561479, BD Biosciences) and PE anti-mouse IL-17A (506904, BioLegend). Cells were acquired on Symphony A5 (BD Biosciences) and analysed using FlowJo v.10 (Becton Dickinson).

### BMDC differentiation

To obtain bone marrow cells, the femurs and tibiae from C57BL/6J mice were removed and obtained by flushing with 1 ml of 0.5% BSA and 2 mM EDTA pH 8.0 in 1 $\times$  PBS. Red blood cells were lysed with ACK lysing buffer (Life Technologies, A10492-01) for 5 min and washed with 0.5% BSA and 2 mM EDTA pH 8.0 in 1 $\times$  PBS. For DC differentiation, cells were cultured in non-adherent petri dishes (100 mm) at 1  $\times$  10<sup>6</sup> cells per ml in DMEM/F12 with GlutaMAX (Life Technologies, 10565042) supplemented with 10% FBS (Life Technologies, 10438026), 1% penicillin-streptomycin (Life Technologies, 15140122), 1% sodium pyruvate (Life Technologies, 11360070), 1% HEPES (Life Technologies, 15630106) and 1% MEM non-essential amino acids (Life Technologies, 11140050) containing 20 ng ml<sup>-1</sup> GM-CSF (PeproTech, 315-03). The medium was replaced on days 3 and 5, and cells were completely differentiated on day 8 and prepared for downstream applications.

### DC stimulation

DCs were treated for 6 h with 100 ng ml<sup>-1</sup> Ultrapure LPS, *E. coli* 0111:B4 (tlrl-3pelps, InvivoGen), 0.1, 1 or 10 mM sodium L-lactate (71718, Sigma-Aldrich), 1 or 10 mM sodium D-lactate (71716, Millipore Sigma), 1.5 mM pyruvate solution (103578-100, Agilent Technologies), 20  $\mu$ M mitoPQ (ab146819, Abcam), 50  $\mu$ M mitoTempo (SML0737, Sigma-Aldrich), 0.1, 0.2 or 1 mM HIF-1 $\alpha$  inhibitor (5655, Tocris Bioscience), 6.5  $\mu$ M dimethyl fumarate (DMF) (242926, Sigma-Aldrich), 10 mM dimethylmalonate (136441-250G, Sigma-Aldrich), 5 mM diethyl succinate (112402, Sigma-Aldrich), 125  $\mu$ M 4-octyl itaconate (3133-16-2, Cayman Chemical Company), 1 mM dimethyl  $\alpha$ -ketoglutarate (349631-5G, Sigma-Aldrich), 10  $\mu$ M ML228 (4565, Tocris Bioscience) and 500  $\mu$ M deferoxamine (D9533-1G, Sigma-Aldrich). In some studies, BMDCs were pre-treated 1 h before stimulation with: 2 mM sodium oxamate (02751, Sigma-Aldrich), 3 mM sodium 3-hydroxybutyrate as a GPR81 antagonist (54965-10G-F, Sigma-Aldrich) and 0.5  $\mu$ M AR-C

141990 hydrochloride (5658, Tocris) or 100 nM AZD3965 (HY-12750, MedChem Express) as MCT1 inhibitors. For cultures under hypoxia, cells were incubated for 6 h in a hypoxia incubator chamber (STEMCELL Technologies, 27310) at 37 °C and 1% CO<sub>2</sub>.

### Human DC and T cell cultures

PBMCs were isolated from healthy blood donors by Ficoll-Paque PLUS density gradient (Sigma-Aldrich, GE17–1440-03). The protocols for this study received prior approval from all institutional review boards, and informed consent was obtained from each individual. Exclusion criteria included pregnancy and having received antibiotics or vaccines within the past three months. DCs were enriched using Pan-DC enrichment kit (130–100-777, Miltenyi), and enriched DCs were stained with BV421 anti-human CD11c (301628, Biolegend), APC Cy7 anti-human HLA-DR (307618, Biolegend) and FITC anti-human CD3 (555232, BD Biosciences). T cells were sorted as CD3<sup>+</sup> cells. DCs sorted as CD3<sup>-</sup>CD11c<sup>+</sup>HLA-DR<sup>+</sup> were silenced and 48-h cells were stimulated with LPS (100 ng ml<sup>-1</sup>) and 10 µg ml<sup>-1</sup> OVA 323–339 (SP-51023–1, Genemed) in the presence of D-LA, L-LA (1 mM) or vehicle. After 6 h, cells were washed, lysed to evaluate cytokine gene expression or co-cultured with allogenic T cells in a 1:10 ratio for 48 h. *HIF1A* was silenced in DCs using the Accell Human *HIF1A*-siRNA smart pool (E-004018–00-0005, Dharmacon). Then, co-cultures of DCs and T cells were performed in the presence of soluble anti-human CD3 (16–0037-85, Thermo Fisher Scientific).

### Knockdown with siRNA

The siRNA pool was mixed with interferin (Polyplus-transfection, 409–10) in Opti-MEM (Life Technologies, 31985062), incubated for 10 min at room temperature and added to pre-plated 200,000 BMDCs. Forty-eight hours later, cells were used for downstream assays. The siRNA pools (1 nM) used were non-targeting siRNA (Dharmacon, D-001810–10-05), *siHif1a* (L-040638–00-0005, Dharmacon), *siHIF1A* (E-004018–00-0005, Dharmacon) *siVhl* (E-040755–00-0005, Dharmacon), *siSlc16a1* (L-058863–01-0005, Dharmacon), and *siNdufa4l2* (L-160257–00-0005, Dharmacon). Knockdown efficiency was confirmed by quantitative PCR (qPCR).

### DC and T cell co-culture

A total of  $3 \times 10^4$  DCs were plated in a Costar low attachment 96-well plate (Sigma-Aldrich, CLS3474–24EA) and stimulated with LPS or LPS + L-LA or D-LA in the presence of 20 µg ml<sup>-1</sup> MOG<sub>35–55</sub> for 6 h. Next, cells were washed with DMEM/F12 + GlutaMAX and co-cultured with  $3 \times 10^5$  naive 2D2<sup>+</sup>CD4<sup>+</sup> T cells for 48 h.

### Recall response

For recall response,  $4 \times 10^5$  splenocytes per well were cultured in complete RPMI medium for 72 h in 96-well plates in the presence of 5, 20 or 100 µg ml<sup>-1</sup> MOG<sub>35–55</sub> (Genemed Synthesis, 110582). During the last 16 h, cells were pulsed with 1 µCi [3H]-thymidine (Perkin Elmer, NET-027A005MC) followed by collection on glass fibre filters (Perkin Elmer, 1450–421) and analysis of incorporated [3H]-thymidine in a β-counter (Perkin Elmer, 1450 MicroBeta TriLux).

## ELISA

Supernatants from splenocytes stimulated with 20  $\mu\text{g ml}^{-1}$  MOG<sub>35–55</sub> peptide (Genemed Synthesis, 110582) for 72 h, or from co-cultures of BMDCs and CD4<sup>+</sup> T cells, were collected to quantify cytokine release by ELISA following the manufacturer's instructions. In brief, Costar 96-well plates (Corning, 3690) were coated with capture antibodies diluted in 1 $\times$  PBS: anti-mouse GM-CSF Capture (Invitrogen, 88–7334-88, 1:250), anti-mouse IL-10 capture (Invitrogen, 88–7105-88, 1:250), purified anti-mouse IFN $\gamma$  (BD Biosciences, 551309, 1:500) and purified anti-mouse IL-17A (BD Biosciences, 555068, 1:500) overnight at 4 °C. Plates were washed twice with 0.05% Tween in 1 $\times$  PBS (Boston BioProducts, IBB-171X) and blocked with 1% BSA in 1 $\times$  PBS (Thermo Fisher Scientific, 37525) for 2 h at room temperature. Standard curve was prepared from cytokine standards diluted in 1 $\times$  Elispot diluent (eBioscience, 00–4202-56). Samples were diluted four times for IFN $\gamma$  and twice for GM-CSF and IL-17A in Elispot diluent, and plated pure for IL-10. Plates were washed twice with 0.05% Tween in 1 $\times$  PBS and samples and standard curve were added and incubated overnight at 4 °C. The next day, plates were washed five times with 0.05% Tween in 1 $\times$  PBS and incubated with detection antibodies diluted in 1 $\times$  Elispot diluent: anti-mouse GM-CSF detection (Invitrogen, 88–7334-88, 1:250), anti-mouse IL-10 detection (Invitrogen, 88–7105-88, 1:250), biotin anti-mouse IFN $\gamma$  (BD Biosciences, 554410, 1:500) and biotin anti-mouse IL-17A (BD Biosciences, 555067, 1:500) shaken for 1 h at room temperature. Afterwards, plates were washed eight times with 0.05% Tween in 1 $\times$  PBS and incubated with Avidin-HRP diluted in 1 $\times$  Elispot diluent (Invitrogen, 88–7334-88, 1:250) shaken for 1 h at room temperature. Next, plates were washed eight times with 0.05% Tween in 1 $\times$  PBS and revealed using 1 $\times$  TMB Substrate Solution (Invitrogen, 00–4201-56). The reaction was stopped by KPL TBM Stop Solution (SeraCare, 5150–0021) and plates were read at 450 nm on a GloMax Explorer Multimode Microplate Reader (Promega).

## Mitochondrial ROS production

A total of  $5 \times 10^5$  BMDCs were stimulated with LPS, L-LA, LPS + L-LA and vehicle for 1 h at 37 °C. Then, cells were stained with 5  $\mu\text{M}$  of mitoSOX mitochondrial indicator (Thermo Fisher Scientific, M36008) for 10 min at 37 °C. Next, cells were washed three times with pre-warmed HBSS and fluorescence was read on a GloMax Explorer Multimode Microplate Reader (Promega).

## Flow cytometry of DCs

To analyse DCs by flow cytometry, CNS, lymph nodes and splenic cell suspensions were incubated with surface antibodies and a live–dead cell marker on ice. After 30 min, cells were washed with 0.5% BSA and 2 mM EDTA in 1 $\times$  PBS, and fixed according to the manufacturer's protocol (eBiosciences, 00–5523-00). Intracellular staining was performed for 1 h at room temperature. The surface antibodies used in this study were: BUV395 anti-mouse MHC-II (17–5321-82, Invitrogen, 1:200), BUV496 anti-mouse CD24 (564664, BD Biosciences, 1:100), BUV563 anti-mouse Ly6G (612921, BD Biosciences, 1:100), BUV661 anti-mouse CD45 (103147, BioLegend, 1:100), BV570 anti-mouse Ly6C (128030, BioLegend, 1:100), BV605 anti-mouse CD80 (563052, BD Biosciences, 1:100), BV650 anti-mouse CD3 (100229, BioLegend, 1:100), BV711 anti-mouse CD8a (100748,

BioLegend, 1:100), BV786 anti-mouse CD11b (101243, BioLegend, 1:100), PE-Texas Red anti-mouse CD11c (117348, BioLegend, 1:100), PE-Cy7 anti-mouse CD4 (100422, BioLegend, 1:100), APC anti-mouse/human CD45R/B220 (103212, BioLegend, 1:100), APC-R700 anti-mouse CD103 (565529, BD Biosciences, 1:100) and APC/Cy7 anti-mouse F4/80 (123118, BioLegend, 1:100). The intracellular antibody used was Alexa Fluor 488 anti-mouse HIF-1 $\alpha$  (BS-0737R-A488, Bioss Antibodies, 1:100). Fluorescence-activated cell sorting (FACS) was performed on a Symphony A5 (BD Biosciences).

### Intracellular flow cytometry analysis of T cells

To analyse T cells, CNS, lymph nodes and splenic cell suspensions were stimulated with 50 ng ml<sup>-1</sup> PMA (Sigma-Aldrich, P8139), 1  $\mu$ M ionomycin (Sigma-Aldrich, I3909–1ML), GolgiStop (BD Biosciences, 554724, 1:1500) and GolgiPlug (BD Biosciences, 555029, 1:1500) diluted in RPMI (Life Technologies, 11875119) containing 10% FBS, 1% penicillin–streptomycin, 50  $\mu$ M 2-mercaptoethanol (Sigma-Aldrich, M6250) and 1% non-essential amino acids (Life Technologies, 11140050). After 4 h, cell suspensions were washed with 0.5% BSA and 2 mM EDTA in 1 $\times$  PBS, and incubated with surface antibodies and a live–dead cell marker on ice. After 30 min, cells were washed with 0.5% BSA and 2 mM EDTA in 1 $\times$  PBS, and fixed using an intracellular labelling kit according to the manufacturer’s protocol (00–5523-00, eBiosciences). The surface antibodies used in this study were: BUV661 anti-mouse CD45 (103147, BioLegend, 1:100), PE-Cy7 anti-mouse CD4 (100422, BioLegend, 1:100), BV750 anti-mouse CD3 (100249, BioLegend, 1:100), BUV395 anti-mouse CD69 (740220, BD Biosciences, 1:100), BUV737 anti-mouse CD11b (564443, BD Biosciences, 1:100), BV805 anti-mouse CD8a (612898, BD Biosciences, 1:100) and PE/Cy5 anti-mouse CD44 (103010, BioLegend, 1:100). The intracellular antibodies were: BV421 anti-mouse GM-CSF (564747, BD Biosciences, 1:100), APC/Cy7 anti-mouse IFN $\gamma$  (561479, BD Biosciences, 1:100) and PE anti-mouse IL-17A (506904, BioLegend, 1:100). Cells were acquired on a Symphony A5 (BD Biosciences) and analysed with FlowJo v.10 (Becton Dickinson).

### RNA isolation

Sorted DCs were lysed in extraction buffer and RNA was isolated following the manufacturer’s instructions (Thermo Fisher Scientific, KIT0204). BMDCs were lysed in RLT Buffer and RNA was isolated using the Qiagen RNeasy Mini kit (Qiagen, 74106). cDNA was transcribed using the High-Capacity cDNA Reverse Transcription Kit (Life Technologies, 4368813). Gene expression was measured by qPCR using Taqman Fast Universal PCR Master Mix (Life Technologies, 4367846). Taqman probes used in this study were: *Gapdh* (Mm99999915\_g1), *Iilb* (Mm00434228\_m1), *Il6* (Mm00446190\_m1), *Iil2a* (Mm00434169\_m1), *Il23a* (Mm00518984\_m1), *Tnf* (Mm00443528\_m1), *Ndufa4l2* (Mm01160374\_g1), *sXbp1* (Mm03464496\_m1), *Xbp1* (Mm00457357\_m1), *Gclm* (Mm01324400\_m1), *Gls* (Mm01257297\_m1), *Phgdh* (Mm01623589\_g1), *Shmt2* (Mm00659512\_g1), *Slc7a11* (Mm00442530\_m1), *Lonp1* (Mm01236887\_m1), *Cox4i1* (Mm0250094\_m1), *Cox4i2* (Mm00446387\_m1), *Hif1a* (Mm00468869\_m1), *Cd36* (Mm00432403\_m1), *Vhl* (Mm00494137\_m1), *Mct1* (Mm01306379\_m1), *Slc2a1* (Mm00441480\_m1), *GAPDH* (Hs02786624\_g1), *IL23A* (Hs00372324\_m1), *IL1B* (Hs01555410\_m1), *IL6* (Hs00174131\_m1), *HIF1A* (Hs00153153\_m1), *IFNG*

(Hs00989291\_m1) and *CSF2* (Hs00929873\_m1). qPCR data were analysed by the ddCt method by normalizing the expression of each gene to *GAPDH* and then to the control group.

### Fluorescent glucose uptake

A total of  $2 \times 10^4$  DCs were stimulated with LPS ( $100 \text{ ng ml}^{-1}$ ) in glucose-free RPMI (11-879-020, Fisher Scientific). After 1 h, cells were washed and stained with  $10 \text{ }\mu\text{M}$  2-NBDG (N13195, Thermo Fisher Scientific) at  $37 \text{ }^\circ\text{C}$ . After 20 min, samples were acquired in a BD LSR Fortessa.

### Quantification of pyruvate

Pyruvate levels were quantified in BMDC lysates after 1 h stimulation using the EnzyChrom pyruvate assay kit (EPYR-100, BioAssay Systems), following the procedure suggested by the manufacturer. The signal was detected on a GloMax microplate reader (Promega).

### Incorporation of lactate

A total of  $2 \times 10^6$  BMDCs were treated with  $1 \text{ mM}$  uniformly labelled  $^{13}\text{C}$ -lactate (CLM-1579-N-0.1MG, Cambridge Isotope Laboratories), in the presence or absence of LPS ( $100 \text{ ng ml}^{-1}$ ). After 1 h, cells were washed with cold  $1 \times \text{PBS}$  and then lysed with  $80\%$  HPLC-grade methanol (34860, Sigma-Aldrich). The analysis of  $^{13}\text{C}$  incorporation into TCA intermediates was performed at the Broad Institute.

### ChIP

Approximately two million BMDCs were processed according to the ChIP-IT Express Enzymatic Shearing and ChIP protocol (Active Motif, 53009) as previously described<sup>55</sup>. In brief, cells were fixed in  $1\%$  formaldehyde for 10 min with gentle agitation, washed in  $1 \times \text{PBS}$ , washed for 5 min in  $1 \times$  glycine stop-fix solution in PBS and scraped in  $1 \times \text{PBS}$  supplemented with  $500 \text{ }\mu\text{M}$  PMSF. Cells were pelleted, the nuclei were isolated, and chromatin sheared using the Enzymatic Shearing Cocktail for 10 min at  $37 \text{ }^\circ\text{C}$ . Sheared chromatin was immunoprecipitated according to the Active Motif protocol overnight at  $4 \text{ }^\circ\text{C}$ , with rotation. The next day, the protein-bound magnetic beads were washed with ChIP buffer 1, ChIP buffer 2 and, finally, with  $1 \times \text{TE}$ . Cross-links were reversed in  $100 \text{ }\mu\text{l}$  of  $0.1\%$  SDS and  $300 \text{ mM}$  NaCl in  $1 \times \text{TE}$  at  $65 \text{ }^\circ\text{C}$  for four to five hours. DNA was purified using the QIAquick PCR Purification Kit (Qiagen, 28104). qPCR was performed using Fast SYBR Green Master Mix (Thermo Fisher Scientific, 4385612). Anti-IgG immunoprecipitation and input were used as controls. The antibodies used were mouse XBP1 (Santa Cruz Biotechnology, SC-8015) and IgG1 isotype control (Abcam, ab171870). PCR primers were designed with Primer3 to generate 50–150-bp amplicons. Primer sequences used: XBP1-IL1B site 1 F:  $5' \text{-CCTGGGCTCTCTGAGTTAGCAGTCTAGTGA-3'}$ ; R:  $5' \text{-AGTGCAAAGGTGGTGAACGAGGCATCTG-3'}$ ; XBP1-IL1B site 2 F:  $5' \text{-GGCTTGCTTCCAGAGTCCCTGACCCTAT-3'}$ ; R:  $5' \text{-GAGTTTGGTAACTGGATGGTGCTTCTGTGC-3'}$ ; XBP1-IL6 site 1 F:  $5' \text{-CCTGCGTTTAAATAACATCAGCTTTAGCTT-3'}$ ; R:  $5' \text{-GCACAATGTGACGTCGTTTAGCATCGAA-3'}$ ; XBP1-IL23 site 1 F:

5'-GCTTCCAACCCTCCAGATCC-3'; R: 3'-ACCTTCCCAGTCCTCCAAGT-5';  
XBP1-IL23 site 2 F: 5'-CCTCTAGCCACAACAACCTC-3'; R: 3'-  
CCTTCACACTAGCAGGTGACT-5'. Data were analysed by ddCt relative to IgG control or  
input DNA.

## OCR

A total of  $3.5 \times 10^5$  *Ndufa4l2*-silenced, non-targeted BMDCs, *Ndufa4l2*-overexpressing BMDCs, wild-type BMDCs or HIF-1 $\alpha$ -deficient BMDCs were plated in Seahorse XF96 Cell Culture Microplates (Agilent Technologies, 101085-004) and stimulated with 10 mM L-LA and 1.5 mM pyruvate, or vehicle for 6 h. OCR was evaluated after treatment with 2  $\mu$ M oligomycin, 1.5  $\mu$ M FCCP and 1  $\mu$ M rotenone/1  $\mu$ M antimycin A (Rot/AA) from the Seahorse XF Cell Mito Stress Test (103015-100, Agilent Technologies), and was read using the Seahorse XFe96 Analyzer (Agilent Technologies).

## Extracellular acidification rate

A total of  $3.5 \times 10^5$  HIF-1 $\alpha$ -deficient or wild-type BMDCs were plated in Seahorse XF96 Cell Culture Microplates (Agilent Technologies, 101085004). Cells were kept in 180  $\mu$ l assay medium (supplemented with 2 mM glutamine, pH 7.4) for one hour. The extracellular acidification rate (ECAR) was determined at the beginning of the assay and after the sequential addition of 10 mM d-glucose, 1  $\mu$ M oligomycin and 100 mM 2-DG. The ECAR was normalized to the total cell number, evaluated with the CyQUANT cell proliferation assay kit (C7026, Invitrogen).

## Luciferase assay

A total of  $4 \times 10^6$  BMDCs from FVB.129S6-Gt(ROSA)26Sortm2(HIF1A/luc)Kael/J mice (006206, The Jackson Laboratory) were stimulated with LPS or LPS + L-LA (10 mM) for 6 h. Next, the luciferase activity was quantified using the Dual-Luciferase Reporter Assay System (Promega, E1910) according to the manufacturer's protocol.

In another set of experiments, HepG2 (ATCC HB-8065) or DC2.4 (SCC142, Millipore) cells were cultured in DMEM supplied with 10% FBS (Gibco) and penicillin-streptomycin (Thermo Fisher Scientific). *Ndufa4l2*- and *Hif1a*-promoter reporter plasmids expressing Gaussia luciferase were acquired from GeneCopoeia. To evaluate *Ndufa4l2* promoter activity cells were stimulated with vehicle, L-LA (10 mM), LPS (100 ng ml<sup>-1</sup>) or the combination of L-LA and LPS. For overexpression assays, *HIF1A* plasmid (OHu27176, GenScript), *Ndufa4l2* plasmid (EX-J0135-M02, GeneCopoeia) or empty control vector (GeneCopoeia) were used. All plasmids were transfected using lipofectamine 2000 (11668019, Thermo Fisher Scientific) following the manufacturer's instructions. Luciferase activity was evaluated with the Gaussia Luciferase Flash Assay Kit (16159, Thermo Fisher Scientific).

## Lactate administration

L-LA or D-LA (125 mg per kg body weight, daily) was administered intraperitoneally, nasally or intravenously starting three days before EAE induction. Tissues were collected 28 days after EAE induction and cell suspensions were used for downstream applications.

## Engineering a D-LA-producing live therapeutic

The strains used in this work are listed in Table 1. *E. coli* Nissle 1917 (EcN), designated as SYN001 here, was originally purchased from the German Collection of Microorganisms and Cell Cultures (DSMZ Braunschweig, *E. coli* DSM 6601). EcN (SYN001) with streptomycin resistance was generated by streaking around  $10^{11}$  cells of SYN001 on an LB plate containing  $300 \text{ ng ml}^{-1}$  streptomycin, followed by considering the single colony formed to have mutated to be streptomycin resistant and designating it as EcN-StrpR (SYN094). The *pta* gene in the pyruvate–acetate pathway was deleted to limit the flux of carbon through acetate production, using the lambda red recombineering technique as described<sup>56</sup>; this resulted in the strain EcN- *pta*. The gene encoding the *E. coli* LdhA protein under the control of a Ptemp promoter was subcloned into a Synlogic vector containing an ampicillin-resistance gene and a low-copy-number origin of replication pSC101. The resulting plasmid was used to electroporate EcN- *pta*, resulting in the strain EcN-lactate.

## Engineering a reporter strain using GFP

The gene encoding GFP, together with an upstream constitutive promoter J23100, was synthesized and subcloned into a Synlogic vector containing an ampicillin-resistance gene and a low-copy-number origin of replication pSC101, resulting in plasmid pSC101-Pconst-rfp-ampR. Then, the gene encoding a GFP under the control of the heat-inducible promoter cassette was synthesized and subcloned into this plasmid pSC101-Pconst-rfp-ampR to obtain the heat-inducible GFP reporter plasmid pSC101-Ptemp-gfp-Pconst-rfp-ampR. This final plasmid was used to transform into EcN to produce EcN-GFP.

## Growth and induction of strains in bioreactors

Cells were inoculated in 50 ml FM1 medium supplemented with  $25 \text{ g l}^{-1}$  glucose in a 500-ml Ultra-Yield flask (Thomson). Cells were grown at  $37 \text{ }^\circ\text{C}$  with shaking at 350 rpm overnight. Next day, 110 ml of the overnight culture was used to inoculate 4 l of FM1 in an Eppendorf BioFlow 115 bioreactor (starting  $\text{OD}_{600 \text{ nm}}$  of around 0.5). The fermenter was controlled at 60% dissolved oxygen and  $30 \text{ }^\circ\text{C}$  with agitation, air and oxygen supplementation, and controlled to pH 7 using ammonium hydroxide. The expression of the *ldhA* gene was induced at an  $\text{OD}_{600 \text{ nm}}$  of around 5 by changing the reactor temperature from  $30 \text{ }^\circ\text{C}$  to  $37 \text{ }^\circ\text{C}$  for 2 h. Cells were collected after 2 h and at an  $\text{OD}_{600 \text{ nm}}$  of around 20. Cells were collected by centrifugation at  $4,500g$  for 30 min at  $4 \text{ }^\circ\text{C}$ , resuspended in formulation buffer and stored at  $-80 \text{ }^\circ\text{C}$ .  $\text{OD}_{600 \text{ nm}}$  was measured on a BioPhotometer Plus spectrophotometer (Eppendorf).

## Protein sequence of the LdhA enzyme used in the plasmid to build the EcN<sup>Lac</sup> strain

MKLAVYSTKQYDKKYLQQVNESFGFELEFFDFLLTEKTAKTANGCEAVCIFVNDDG  
SRPVLEELKKHGKVKYIALRCAGFNNVDLDAAKELGLKVVRVPAYDPEAVAEHAIGM  
MMTLNRRIHRAYQRTRDANFSLEGLTGFTMYGKTAGVIGTGKIGVAMLRILKGFGM  
RLLAFFDPYPSAAALELGVYVDLPTLFSESDVISLHCPLTPENYHLLNEAAFEQMKN  
GVMIVNTSRGALIDSQAAIEALKNQKIGSLGMDVYENERDLFFEDKSNQVQDDVFR  
RLSACHNVLFTHGQAFLEALTSISQTTLQNLNLEKGETCPNELV.

**DNA sequence of plasmid pSC101-Ptemp-ldhA-ampR**

aaaaatgaagttttaaactcaatctaaagtatatatagtaaaacttggtctgacagttaccaatgcttaacagtgaggcacctatctcagc  
 gatctgtctatttcgtccatcatagttgcctgactccccgtcgtgtagataactacgatacgggagggttaccatctggccccagtgct  
 gcaatgataaccgcgagaaccagctcaccggctccagattatcagcaataaaccagccagccggaaggccgagcgcagaagt  
 ggtcctgcaactttatccgcctccatccagctcttaataattgttgcgggaagctagagtaagtagttcccgacttaataagtttgcgcaacg  
 ttgttgcattgctacaggcatcgtggtgtcacgctcgtcgtttggtatggcttcattcagctccggttccaacgatcaagcgcagttac  
 atgatccccatggtgtcaaaaaagcggtagctcttcggtcctccgacgttgcagaagtaagttggccgcagtggtatcactcat  
 ggttatggcagcactgcataattctctactgtcatgccatccgtaagatgcttttctgtgactggtgagtactcaaccaagtcattctgag  
 aatagtgtatgcggcgaccgagttgctcttccccggcgtcaatacgggataataccgcccacatagcagaactttaaagtgctcat  
 cattggaaaacgttctcggggcgaactctcaaggatctaccgctgttgagatccagttcagatgaaccactcgtgcaccaact  
 gatcttcagcatcttttactttaccagcgtttctgggtgagcaaaaacaggaaggcaaaatgccgcaaaaaagggaataaggcgga  
 cacggaatgtgaatactcactcttctttcaatattatgaagcattatcagggttattgtctcatgagcggatacatattgaatgt  
 atttagaaaaataacaataggggtccgcgcacattccccgaaaagtgccacctgacgtctagaaccattattatcatgacatta  
 acctataaaaatagggctatcacgaggcccttctcgcgcggttccggtgatgacggtgaaaacctctgacacatgcagctccccg  
 agacggcacagcttctgtgaagcggatgccgggagcagacaagcccgtcaggggcgcgtcagcgggtgttggcgggtgtcggg  
 gctggcttaactatgcggcatcagagcagattgtactgagagtgaccatatgcgggtgaaataccgcacagatcgtgaaggagaa  
 aataccgcatcagggccattcgcattcaggctgcgcaactgttgggaaggcgcagcgggtcgggctcttcgctattacgccagc  
 tggcgaagggggatgtgctcaagcgcattaaagtgggtaacgccagggtttccagtcacgacgttgaaaacgacggccagt  
 gcgCTCCCGGAGACGGTACAGCTTGTCaaaaaaaaccccgttcggcggggttttttGGTACCT  
 CATCAGCCAAACGTCTCTTCAGGCCACTGACTAGCGATAACTTTCCCAACAACGG  
 AACAACTCTCATTGCATGGGATCATTGGGTACTGTGGGTTTAGTGGTTGTAAAAAC  
 ACCTGACCGCTATCCCTGATCAGTTTCTTGAAGGTAAACTCATCACCCCAAGTCT  
 GGCTATGCAGAAATCACCTGGCTCAACAGCCTGCTCAGGGTCAACGAGAATTAAC  
 ATTCCGTCAGGAAAGCTTGGCTTGGAGCCTGTTGGTGCGGTCATGGAATTACCTT  
 CAACCTCAAGCCAGAAT  
 GCAGAATCACTGGCTTTTTTTGGTTGTGCTTACCCATCTCTCCGCATCACCTTTGGT  
 AAAGGTTCTAAGCTTAGGTGAGAACATCCCTGCCTGAACAT-  
 GAGAAAAACAGGGTACTCATACTCACTTCTAAGTGACGGCTGCATACTAACC GC  
 TTCATACATCTCGTAGATTTCTCTGGCGATTGAAGGGCTAAATTCTTCAACGCTAA  
 CTTTGAGAATTTTTGTAAAGCAATGCGGCGTTATAAGCATTTAATGCATTGATGCCAT  
 TAAATAAAGCACCAACGCCTGACTGCCCATCCCATCTTGTCTGCGACAGATTCC  
 TGGGATAAGCCAAGTTCATTTTTCTTTTTTCATAAATTGCTTTAAGGCGACGTGC  
 GTCCCTCAAGCTGCTCTTGTGTTAATGTTTCTTTTTTTGTGCTCATACTTAAATCTA  
 TCACCGCAAGGGATAAATATCTAACACCGTGCGTGTGACTATTTTACCTCTGGCG  
 GTGATAATGGTTGCATaagtgaggatcaaaagtaactctagaataattttgttaactttaagaaggagtatacatAT  
 GAAACTTGCTGTATATAGTACCAAACAGTACGACAAAAAGTACCTTCAACAGGTC  
 AACGAGAGCTTTGGTTTTCGA ACTTGAATTTTTCGACTTTTTACTTACCGAGAAAAC  
 GGCAAAAACGGCGAACGGATGTGAAGCGGTTTGCATTTTCGTCAACGACGACGG  
 CAGCCGCCCTGTTTTAGAAGAGTTAAAGAAACATGGAGTTAAATACATCGCATTAC  
 GTTGTGCAGGTTTCAACAACGTTGATCTGGATGCTGCGAAGGA ACTGGGATTGAA  
 AGTTGTGCGCGTGCCCGCTTATGACCCAGAGGCGGTTGCGGAACACGCTATTGGT  
 ATGATGATGACCCTTAATCGTCGCATCCATCGTGCATATCAGCGCACGCGGATGC  
 TAACTTCAGTTTAGAAGGATTAACGGGATTTACAATGTACGGGAAGACCGCTGGC  
 GTGATTGGCACCGGAAAAATCGGTGTGGCAATGCTGCGTATCTTGAAGGGGTTTG  
 GCATGCGTTTTGTTAGCATTTGATCCCTATCCAAGTGCCCGGCCCTGGA ACTGGGA

Author Manuscript

Author Manuscript

Author Manuscript

Author Manuscript

GTGGAATATGTTGATTTGCCAACTTTGTTTAGCGAGTCCGATGTTATCTCATTGCAT  
 TGTCCACTTACTCCGGAGAATTATCATTATTGAATGAAGCCGCCTTCGAACAAAT  
 GAAAAATGGAGTGATGATCGTAAATACAAGTCGTGGCGCGTTGATCGATTTCGAG  
 GCAGCGATCGAAGCGTTAAAAAATCAAAGATTGGATCACTGGGCATGGATGTCT  
 ATGAAAACGAGCGCGACCTTTTCTTTGAAGACAAAAGTAATGATGTTATCCAAGA  
 TGATGTATTTCCGCCGTCTGTCCGCATGCCATAATGTACTTTTTACGGGTACCAAGC  
 ATTCCTTACTGCCGAGGCTCTGACTAGCATTTCACAAACCACTCTTCAGAATCTTT  
 CAAATCTTGAGAAAGGTGAGACGTGCCCAATGAATTGGTTaaGCATGCTAATCA  
 GCCGTGGAATTCGGTCTCaGGAGgtacgcatggcatggatgaccgatgtagtggggctctcccatgcgaga  
 gtagggaactgccagcatcaataaaacgaaggctcagtcgaaagactgggcttctgtttatctgtgtttgctggtgaacgctc  
 cctgagtaggacaaatccggcgaggcggattgaacgttgcgaagcaacggccggagggtggcggcaggacgccgcat  
 aaactgccagcatcaataaagcagaaggccatctgacggatggccttttgcgtggccagtccaagctgcatgctgccagc  
 tgcattaatgaagaatcatgctggaagaataacagctcactcaaaaggcggtagtacgggtttgctcccgaacggctgttctg  
 gtgtgctagtgttatcagaatgcagatccggctcagccggttgcggctgaaagcgctatttctccagaattgccatgattttc  
 cccacgggagcgtcactggctcccgtgttgcggcagctttgatcgataagcagcatgcctgttccaggctgctatgtgtgactgt  
 tgagctgaacaagttgctcaggtgtcaattcatgttctagtgtcttgtttactggttccactgttctattagggtgtacatgctgtcat  
 ctgttacattgctgatctgttcatggtgaacagcttgaatgcacaaaaactcgtaaaagctctgatgtatctatcttttacaccgtttca  
 tctgtgcatatggacagtttcccttgatagtaacggtgaacagttgttctactttgtttgtagcttctgatgcttactgatagatacaag  
 agccataagaacctcagatcctccgtatttagccagatgttctctagtgtggtcgtgttttgcgtgagccatgagaacgaaccattg  
 agatcactacttgcagctcactcaaaaatgttgcctcaaaactggtgagctgaattttgcagttaaagcagcgtgtagtgttttcttag  
 tccgttatgtaggtagaaatctgatgtaatggtgtgtgattttgaccattcattttatctggtgttctcaagttcggttacgagatccat  
 ttgctatctagttcaacttggaaaatcaacgtatcagtcggcgccctcgtatcaaccaccaatctatattgctgtaagtgtttaaact  
 tttactattggttcaaaccttggtaagccttttaactcatgtagtattttcaagcattaaactcaactaaatcatcaaggctaat  
 ctctatattgctgtgagtttctttgtgttagtcttttaataaccactataaatcctcatagagtattgtttcaaaagacttaacatgttc  
 cagattatattttatgaatttttaactggaagataaggcaatatcttcaactaaaactaattctaattttcgttgagaactggcata  
 gttgtccactggaataatcgaagcctttaaaccaaaggattcctgatttccacagttctcgtcatcagctctctggttgccttagctaatac  
 accataagcatttccctactgatgttcatcatctgagcgtattggtataagtgaacgataaccgtccgttcttcttctgtaggggtttcaatc  
 gtggggtgtagtagtccacacagcataaaatagcttggttcatgctccgttaagtcatagcgaactaatcgtagttcatttgcctttaa  
 acaactaactcagacatacatcaattggtctaggtgatttaactactataccaattgagatgggctagtcgaatgataaactactagctct  
 tttcctttagttgtgggtatctgaaattctgtagaccttctgctgaaaactgtaaaactctgtagacctctgtaaaactccgctaga  
 cctttgtgtgtttttgtttatattcaagtgttataattatagaataaagaataaaaaaagataaaaaaagataaaagaaatagatcccagcctg  
 gtataactcactttagtcagttccgcagttacaaaaggatgtcgaaacgctgtttgctcctctacaaaacagaccttaaaacc  
 taaaggcttaagtagcaccctcgaagctcgggcaaatcgtgaatattcctttgtctccgaccatcagccactgagtcgctgtctttt  
 tctgacattcagttcgtcgtcagcggctctggcagtgatgggggtaaatggcactacagggcctttatggattcatgcaaggaa  
 aactaccataatacaagaaaagcccgtcacgggctctcagggcggtttatggcgggtctgctatgtggtgctatctgacttttctgt  
 tcagcagttctgacctgattttccagctgaccactcggattatcccgtgacaggt  
 cattcagactggcgaatgcaccagtaaggcagcggatcatcaaacggcttaccgtcttactgtcttttctacggggtctgacgctca  
 gtggaacgaaaactcacgttaagggttttggatgagattatcaaaaggatcttccctacctagatccttttaaat.

### DNA sequence of plasmid pSC101-Ptemp-gfp-Pconst-rfp-ampR

cAACTTAGCGGTAAACCTCGTTGCCACCTACTGTCAGACCAAGTTACTCATATATA  
 CTTTAGATTGATTTAAACTTCATTTTTTAATTTAAAGGATCTAGGTGAAGATCCTT  
 TTTGATAATCTCATGACCAAAATCCCTAACGTGAGTTTTCGTTCCACTGAGCGTC  
 AGACCCCGTAGAAAAGACAGTAAGACGGGTAAGCCTGTTGATGATACCGCTGCCT  
 TACTGGGTGCATTAGCCAGTCTGAATGACCTGTCACGGGATAATCCGAAGTGGTC

AGACTGGAAAATCAGAGGGCAGGAACTGCTGAACAGCAAAAAGTCAGATAGCAC  
CACATAGCAGACCCGCCATAAAACGCCCTGAGAAGCCCGTGACGGGCTTTTCTTG  
TATTATGGGTAGTTTCCTTGCATGAATCCATAAAAGGCGCCTGTAGTGCCATTTACC  
CCCATTCACTGCCAGAGCCGTGAGCGCAGCGAACTGAATGTCACGAAAAAGACA  
GCGACTCAGGTGCCTGATGGTCCGAGACAAAAGGAATATTCAGCGATTTGCCCGA  
GCTTGCAGGGTGTACTTAAGCCTTTAGGGTTTTAAGGTCTGTTTTGTAGAGGAG  
CAAACAGCGTTTGCACATCCTTTTGTAACTGCGGAACTGACTAAAGTAGTGA  
GTTATACACAGGGCTGGGATCTATTCTTTTTATCTTTTTTTATTCTTTCTTTATTCTAT  
AAATTATAACCACTTGAATATAAACAACAAAAACACACAAAGGTCTAGCGGAATT  
TACAGAGGGTCTAGCAGAATTTACAAGTTTTCCAGCAAAGGTCTAGCAGAATTTAC  
AGATACCCACAACCTCAAAGGAAAAGGACTAGTAATTATCATTGACTAGCCCATCTC  
AATTGGTATAGTGATTAATAACCTAGACCAATTGAGATGTATGTCTGAATTAGTT  
GTTTTCAAAGCAAATGAACTAGCGATTAGTCGCTATGACTTAACGGAGCATGAAAC  
CAAGCTAATTTTATGCTGTGTGGCACTACTCAACCCACGATTGAAAACCCTACAA  
GGAAAGAACGGACGGTATCGTTCACCTATAACCAATACGCTCAGATGATGAACATC  
AGTAGGGAAAATGCTTATGGTGTATTAGCTAAAGCAACCAGAGAGCTGATGACGA  
GAACTGTGGAAATCAGGAATCCTTTGGTTAAAGGCTTTGAGATTTTCCAGTGGAC  
AACTATGCCAAGTTCTCAAGCGAAAAATTAGAATTAGTTTTTAGTGAAGAGATAT  
TGCCTTATCTTTTCCAGTTAAAAAAATTCATAAAATATAATCTGGAACATGTAAAGT  
CTTTTGAAAACAATACTCTATGAGGATTTATGAGTGGTTATTAAGAAGCTAACA  
CAAAAGAAAACCTACAAGGCAAATATAGAGATTAGCCTTGATGAATTTAAGTTCAT  
GTTAATGCTTGAAAATAACTACCATGAGTTTTAAAAGGCTTAACCAATGGGTTTTGA  
AACCAATAAGTAAAGATTTAAACACTTACAGCAATATGAAATTGGTGGTTGATAAG  
CGAGGCCGCCGACTGATACGTTGATTTTCCAAGTTGAACTAGATAGACAAATGG  
ATCTCGTAACCGAACTTGAGAACAACCAGATAAAAATGAATGGTGACAAAATACC  
AACCAACCATTACATCAGATTCCTACCTACGTAACGGACTAAGAAAAACTACACG  
ATGCTTTAACTGCAAAAATTCAGCTCACCAGTTTTGAGGCAAAATTTTTGAGTGAC  
ATGCAAAGTAAGCATGATCTCAATGGTTCGTTCTCATGGCTCACGCAAAAACAAC  
GAACCACACTAGAGAACATACTGGCTAAATACGGAAGGATCTGAGGTTCTTATGGC  
TCTTGATCTATCAGTGAAGCATCAAGACTAACAACAAAAGTAGAACAACCTGTTCC  
ACCGTTAGATATCAAAGGGAAAACCTGTCCATATGCACAGATGAAAACGGTGTAAA  
AAAGATAGATACATCAGAGCTTTTACGAGTTTTTGGTGCATTTAAAGCTGTTACC  
ATGAACAGATCGACAATGTAACCTCCTTCGTTGAGAACTACAATTATATTACC  
AATGCTTAATCAGTGAGGCACCTATCTCAGCGATCTGTCTATTTTCGTTTCATCCATAG  
TTGCCCTGACTCCCCGTCGTGTAGATAACTACGATACGGGAGGGCTTACCATCTGGC  
CCCAGTGCTGCAATGATACCGGAGACCCACGCTCACCGGCTCCAGATTTATCAG  
CAATAAACCAGCCAGCCGGAAGGGCCGAGCGCAGAAGTGGTCTGCAACTTTAT  
CCGCCTCCATCCAGTCTATTAATTGTTGCCGGGAAGCTAGAGTAAGTAGTTCGCCA  
GTTAATAGTTTGCACAACGTTGTTGCCATTGCTACAGGCATCGTGGTGTACAGCTC  
GTCGTTTGGTATGGCTTCATTCAGCTCCGGTTCCTAACGATCAAGGCGAGTTACAT  
GATCCCCCATGTTGTGCAAAAAGCGGTTAGCTCCTTCGGTCTCCGATCGTTGT  
CAGAAGTAAGTTGGCCGAGTGTATCACTCATGGTTATGGCAGCACTGCATAATT  
CTCTTACTGTGATGCCATCCGTAAGATGCTTTTTCTGTGACTGGTGAGTACTCAACC  
AAGTCATTCTGAGAATAGTGTATGCGGCGACCGAGTTGCTCTTGCCCGGCGTCAA  
TACGGGATAATACCGCGCCACATAGCAGAACTTTAAAAGTGCTCATCATTGGAAAA

CGTTCTTCGGGGCGAAAACCTCTCAAGGATCTTACCGCTGTTGAGATCCAGTTTCGA  
 TGTAACCCACTCGTGCACCCAACCTGATCTTCAGCATCTTTTACTTTACCCAGCGTT  
 TCTGGGTGAGCAAAAACAGGAAGGCAAAATGCCGCAAAAAGGGAATAAGGGC  
 GACACGGAAATGTTGAATACTCATACTCTTCCTTTTTCAATATTATTGAAGCATTTA  
 TCAGGGTTATTGTCTCATGAGCGGATACATATTTGAATGTATTTAGAAAAATAACA  
 AATAGGGGTTCCGCGCACATTTCCCCGAAAAGTGCCACCTGACGTCTAAGAAACC  
 ATTATTATCATGACATTAACCTATAAAAATAGGCGTATCACGAGGCCCTTTCGTCTC  
 GCGCGTTTTCGGTGATGACGGTGAAAACCTCTGACACATGCAGCTCCCGGAGACG  
 GTCACAGCTTGTCAACAAGACCTGACCTAACGGTAAGAttattaagcaccggtggagtacgacc  
 ttcagcacgttcgactgttcaacgatggtgtagcttcgtggtggaggatggtccagtttgatgctggtttgtaagcaccggcagc  
 tgaaccggttttagccatgtaggtggtttaactcagctcgtgtagtaccaccgtcttcagtttcagacgcattttgattcaccttca  
 gagcaccgtctccgggtacatacgttcggtggaagctcccaaccatggtttttctgcataaccggaccgtcggacgggaagttg  
 gtaccacgcagtttaactttgtagatgaactcaccgtcttcgagggaggagtctgggtaacggttaacaacaccaccgtcttcgaagt  
 cataacacgttccatttgaacctccgggaaggacagtttcaggtagtcgggatgtagccgggtgttaacgtaagctttggaac  
 cgtactggaactgcggggacaggtatcccaagcgaacggcagcggaccactttgtaactttagcgtttagcggctcgggtacctt  
 cgtacggacgaccttcaccttcaccttcgatttcgaactcgtgaccgttaacggaacctccatacgaactttgaaacgcatagaactctt  
 gataacgtcttcggaggaaaccatctagcttctctgtgtagcttagtagtagcactgtacttaggactgagctagccgtcaaAC  
 GATTGGTAAACCCGGTgaacgatgagAAAGCCCCGGAAGATCACCTTCCGGGGGCT  
 TTTttattgGcGGACCAAACGAAAAAAGACGCTCGAAAGCGTCTCTTTTTCTGGAATT  
 TGGTACCGAGCATTTCGATCAGCCAAACGTCTCTTCAGGCCACTGACTAGCGATAAC  
 TTTCCCCACAACGGAACAACCTCTCATTGCATGGGATCATTGGGTACTGTGGGTTTA  
 GTGGTTGTAAAAACACCTGACCGCTATCCCTGATCAGTTTCTTGAAGGTAAACTCA  
 TCACCCCAAGTCTGGCTATGCAGAAATCACCTGGCTCAACAGCCTGCTCAGGGT  
 CAACGAGAATTAACATTCCGTCAGGAAAGCTTGGCTTGGAGCCTGTTGGTGCGGT  
 CATGGAATTACCTTCAACCTCAAGCCAGAATGCAGAATCACTGGCTTTTTTTGGTTG  
 TGCTTACCCATCTCTCCGCATCACCTTTGGTAAAGGTTCTAAGCTTAGGTGAGAAC  
 ATCCCTGCCTGAACATGAGAAAAACAGGGTACTCATACTCACTTCTAAGTGACG  
 GCTGCATACTAACCGCTTCATACATCTCGTAGATTTCTCTGGCGATTGAAGGGCTA  
 AATTCTTCAACGCTAACTTTGAGAATTTTGTAAAGCAATGCGGGCTTATAAGCATT  
 TAATGCATTGATGCCATTAATAAAGCACCAACGCTGACTGCCCCATCCCCATCT  
 TGTCTGCGACAGATTCCTGGGATAAGCCAAGTTCATTTTTCTTTTTTTCATAAATTG  
 CTTTAAAGGCGACGTGCGTCTCAAGCTGCTCTTGTGTTAATGGTTTCTTTTTTGTG  
 CTCATACGTTAAATCTATCACCGCAAGGGATAAATATCTAACACCGTGCGTGTGA  
 CTATTTTACCTCTGGCGGTGATAATGGTTGCATagctgtcaccggatggtctccggctgatgagtcggt  
 gaggacgaaacagcctctacaataattttgtaaaACAACACCCACTAAGATAAGGTAGAAACATGA  
 GCAAAGGAGAAGAACTTTTACTGGAGTTGTCCCAATTCTTGTGTAATTAGATGG  
 TGATGTTAATGGGCACAAATTTTCTGTCCGTGGAGAGGGTGAAGGTGATGCTACA  
 AACGAAAACCTCACCTTAAATTTATTTGCACTACTGGAAAACCTACCTGTTCCGTG  
 GCCAACACTTGTCACTACTCTGACCTATGGTGTTCAATGCTTTTCCCGTTATCCGG  
 ATCACATGAAACGGCATGACTTTTTCAAGAGTGCCATGCCGAAGGTTATGTACAG  
 GAACGCACTATATCTTTCAAAGATGACGGGACCTACAAGACGCGTGCTGAAGTCA  
 AGTTTGAAGGTGATACCCTTGTTAATCGTATCGAGTTAAAGGGTATTGATTTAAAG  
 AAGATGGAAACATTCTTGGACACAACTTGAGTACAACCTTAACTCACACAATGT  
 ATACATCACGGCAGACAAACAAAAGAATGGAATCAAAGCTAACTTCAAATTCGC  
 CACAACGTTGAAGATGGTTCCGTTCAACTAGCAGACCATTATCAACAAAATACTCC

AATTGGCGATGGCCCTGTCCTTTTACCAGACAACCATTACCTGTCGACACAATCTG  
TCCTTTCGAAAGATCCCAACGAAAAGCGTGACCACATGGTCCTTCTTGAGTTTGT  
AACTGCTGCTGGGATTACACATGGCATGGATGAGCTCTACAAATGAgttggtctggtgca  
aaataaCTCaatagGTCGACagttaacaaAAAGGGGGGATTTTATCTCCCCTTTaatcttctGTC  
TCCCcctttggtcgAAAAAAAAAGCCCGCACTGTCAGGTGCGGGCTTTTTTctgtgttccCT  
TGAAGTAATGTATACGACAGAGTCCGTGCACCTACCAA.

### Bacterial genome sequencing

Bacterial genomic DNA from each strain was purified individually using the QIAamp Fast DNA Stool Mini Kit (Qiagen, 51604). DNA was quantified by Nanodrop. Input DNA (250 ng) was prepared for sequencing using the NEBNext Ultra II DNA Library Prep Kit (New England Biolabs, E7645S) and sequencing adaptors were ligated using NEBNext Multiplex Oligos for Illumina (E7500S and E7335S) as described. Bacterial DNA was amplified by using four cycles according to the NEBNext protocol. Libraries were quantified using a Library Quantification Kit (Kapa Biosystems, KK4824) and sequenced on a NextSeq550 High Output. Deep-sequencing reads were then aligned to the CP022686.1 reference genome for *E. coli* Nissle 1917.

### D-LA production kinetics

To validate D-LA-producing bacteria in vivo, control bacteria and EcN<sup>Lac</sup> were administered by oral gavage for a week. One, four and twenty-four hours after the last gavage, plasma was collected in heparinized tubes and faecal content from the small intestine and colon was collected in BeadBug prefilled tubes (Millipore Sigma, Z763829), weighted and diluted in 0.5 ml cold and sterile 1× PBS. Next, samples were homogenized in PowerLyzer 24 Homogenizer (Qiagen, 13155) twice at 4 m s<sup>-1</sup> for 10 s, and then, at maximal speed for 20 min at 4 °C. Supernatants were used to quantify CFU and the levels of D-LA and L-LA. In another set of experiments, the small intestine and colon were isolated 1, 4 and 24 h after D-LA bacteria gavage, and digested for flow cytometry analysis. To evaluate the protective role of EcN<sup>Lac</sup>, control or EcN<sup>Lac</sup> bacteria were gavaged every day starting three days before EAE induction or weekly starting on the day of EAE induction.

### Quantification of D-LA and L-LA

For D-LA, faeces and plasma were filtered on a 10kD Spin Column (Abcam, ab93349) to concentrate D-LA. For L-LA, samples were deproteinized by PEG precipitation. The concentrations of D-LA and L-LA were quantified using the D-Lactate Assay Kit (Abcam, ab174096) and L-lactate Assay Kit (Biomedical Research, Service and Clinical Application A-108) as per the manufacturer's instructions.

### CFU

Faeces supernatants were serially diluted and seeded in LB Agar medium with 300 µg ml<sup>-1</sup> of streptomycin for control bacteria (Syn094) or 100 µg ml<sup>-1</sup> of carbenicillin–ampicillin for D-LA-producing bacteria (Syn028). Next day, formed colonies were counted and the dilution factor was corrected.

### Inducible activation analysis in vitro

D-LA-producing bacteria or GFP<sup>+</sup> bacteria (SYNB2189) were diluted in 2× YT medium (Sigma-Aldrich, Y1003–500ML) with 100 µg ml<sup>-1</sup> of carbenicillin–ampicillin or 100 µg ml<sup>-1</sup> of carbenicillin, respectively, and shaken at 250 rpm at 37 °C. At the indicated time points, D-LA was quantified as previously described, and GFP expression was measured by FACS on a Symphony A5 (BD Biosciences).

### Sorting of mouse DCs

cDCs from the CNS and spleen were sorted as B220<sup>-</sup>Ly6G<sup>-</sup>Ly6C<sup>-</sup>TER119<sup>-</sup>O4<sup>-</sup>CD45<sup>high</sup>CD11c<sup>high</sup>MHCII<sup>high</sup>. Compensation was performed on single-stained beads. Cells were sorted on a FACS Aria Ilu (BD Biosciences).

### Bulk RNA-seq

Sorted cells were lysed in extraction buffer and RNA was isolated using the PicoPure RNA Isolation Kit (Thermo Fisher Scientific, KIT0204). RNA was suspended in 10 µl nuclease-free water at a concentration of 0.5–1 ng µl<sup>-1</sup> and was sequenced using Smart-Seq2 (ref. 57) at the Broad Institute. All bulk RNA-seq results were aligned to the Ensembl GRCm38. p6 reference genome and quantified using Kallisto (v.0.46.1)<sup>58</sup> and Salmon (v. 1.1.0)<sup>59</sup>. DESeq2 software was used to perform differential expression analysis and the apeGLM algorithm<sup>60</sup> was used to remove noise in log<sub>2</sub>-transformed fold-change analyses after differential expression analysis.

### Pathway analysis

GSEA or GSEAPreranked analyses were used to generate enrichment plots for bulk RNA-seq or scRNA-seq data<sup>61,62</sup> using MSigDB molecular signatures for canonical pathways: KEGG/Reactome/Biocarta (c2.cp.all), Motif (c3.all), Gene Ontology (c5.cp.all) and Hallmark (h.all). To determine regulators of gene expression networks, Ingenuity Pathway Analysis software (Qiagen) was used by inputting gene expression datasets with corresponding log(fold change) expression levels compared to other groups. ‘Canonical pathways’ and ‘upstream analysis’ metrics were considered significant at  $P < 0.05$ .

### Tissue immunofluorescence

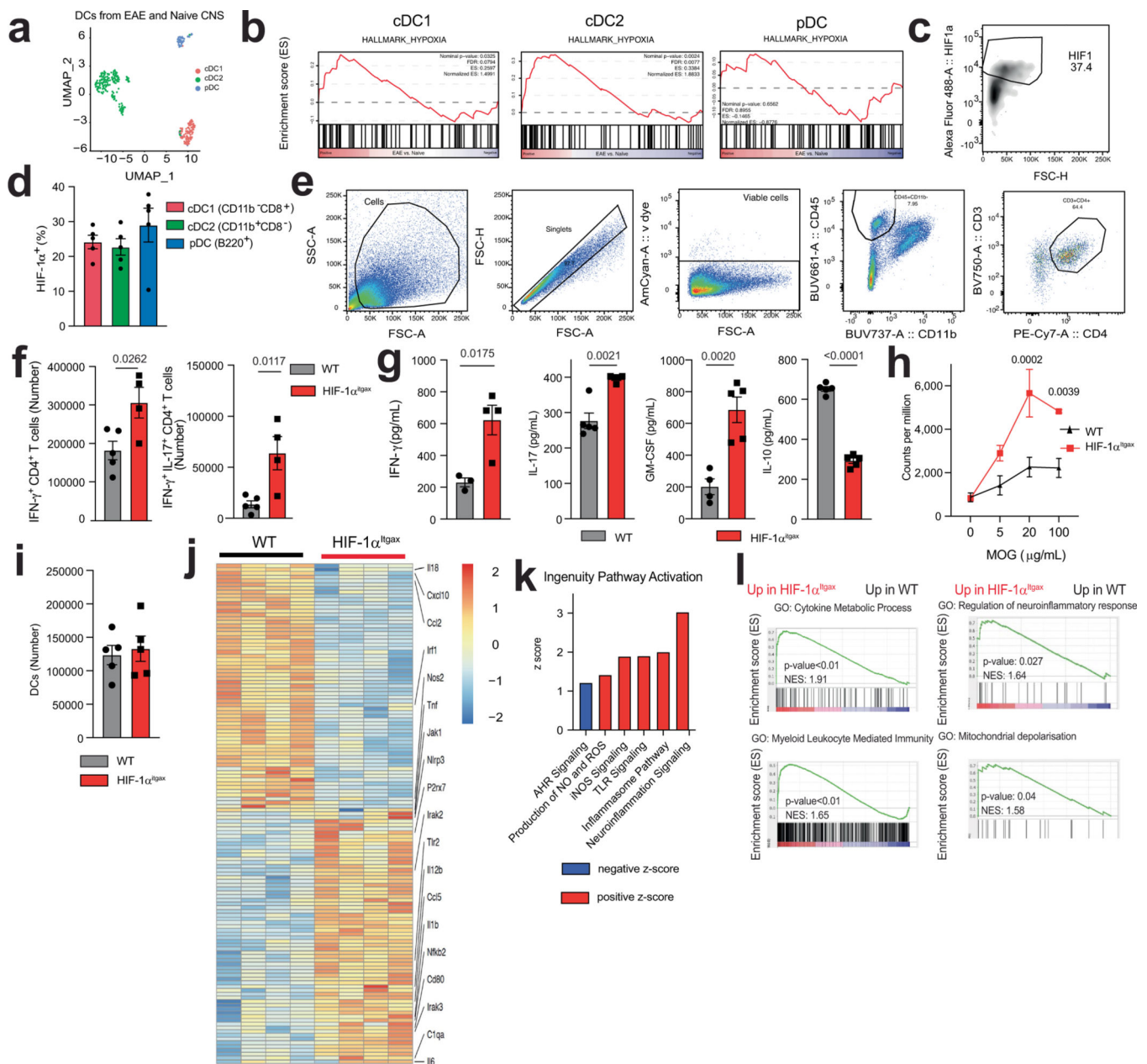
For immunofluorescence, distal ileum and distal colon were dissected after one week of EcN or EcN<sup>Lac</sup> treatment, then fixed in 4% paraformaldehyde for 4 h at 4 °C. Tissue was subsequently dehydrated by incubating in 10% sucrose in PBS for 1 h at 4 °C, then 20% sucrose in PBS for 1 h at 4 °C, then 30% sucrose overnight at 4 °C. Tissues were frozen in OCT (Sakura, 4583) and 8-µm sections were prepared by cryostat on SuperFrost Plus Gold slides (Fisher Scientific, 15–188-48). Sections were permeabilized with 1× permeabilization buffer (BD Biosciences, 554723) for 10 min at room temperature, then blocked using serum-free protein block (Agilent, X0909) for 10 min at room temperature. Sections were then incubated with primary antibodies diluted in 1× permeabilization buffer overnight at 4 °C. After incubation with primary antibodies, sections were washed three times with 1× permeabilization buffer and incubated with secondary or conjugated antibodies diluted in 1× permeabilization buffer for 1 h at room temperature. After incubation with secondary

and conjugated antibodies, sections were washed three times with 1× permeabilization buffer and mounted with ProLong Gold Antifade Mountant (Fisher Scientific, P36930). The primary and conjugated antibodies used in this study were: Armenian hamster anti-CD11c Pacific Blue (Biolegend, 1:100, 117321), goat anti-HIF-1 $\alpha$  (R&D Systems, 1:100, AF1935-SP), rabbit anti-NDUFA4L2 (Proteintech, 1:50, 16480-1-AP) and mouse anti-sXBP1 (Biolegend, 1:50, 647502). The secondary antibodies used in this study were: donkey anti-goat IgG Alexa Fluor 488 (Jackson ImmunoResearch, 705-545-003), donkey anti-rabbit IgG (H+L) highly cross-adsorbed, Alexa Fluor 568 (Life Technologies, A10042) and donkey anti-mouse IgG H&L, Alexa Fluor 647 (Abcam, ab150107), all at 1:1,000 working dilution. Sections were imaged and tile scan images were stitched on an LSM-880-AiryScan confocal microscope using the ZEN Black software (Zeiss), and image analysis was performed with the Fiji version of ImageJ (NIH). The expression of HIF1- $\alpha$ , NDUFA4L2 and sXBP1 in DCs in sections of the colon and small intestine was quantified as previously described<sup>63,64</sup>. In brief, CD11c<sup>+</sup> cells were detected by implementing the bwlabel algorithm for labelling connected components in two-dimensional images<sup>65</sup> using MATLAB (MathWorks). Small puncta (less than 50  $\mu\text{m}^2$ ) were regarded as artefacts and were filtered out. Blood-vessel-related fluorescence artefacts were manually removed. Next, the averaged HIF1- $\alpha$ , NDUFA4L2 and sXBP1 fluorescence intensities were calculated per individual CD11c-positive cells and outliers were removed using the robust regression and outlier removal (ROUT) method with coefficient  $Q = 1\%$  (ref. 66).

### Reporting summary

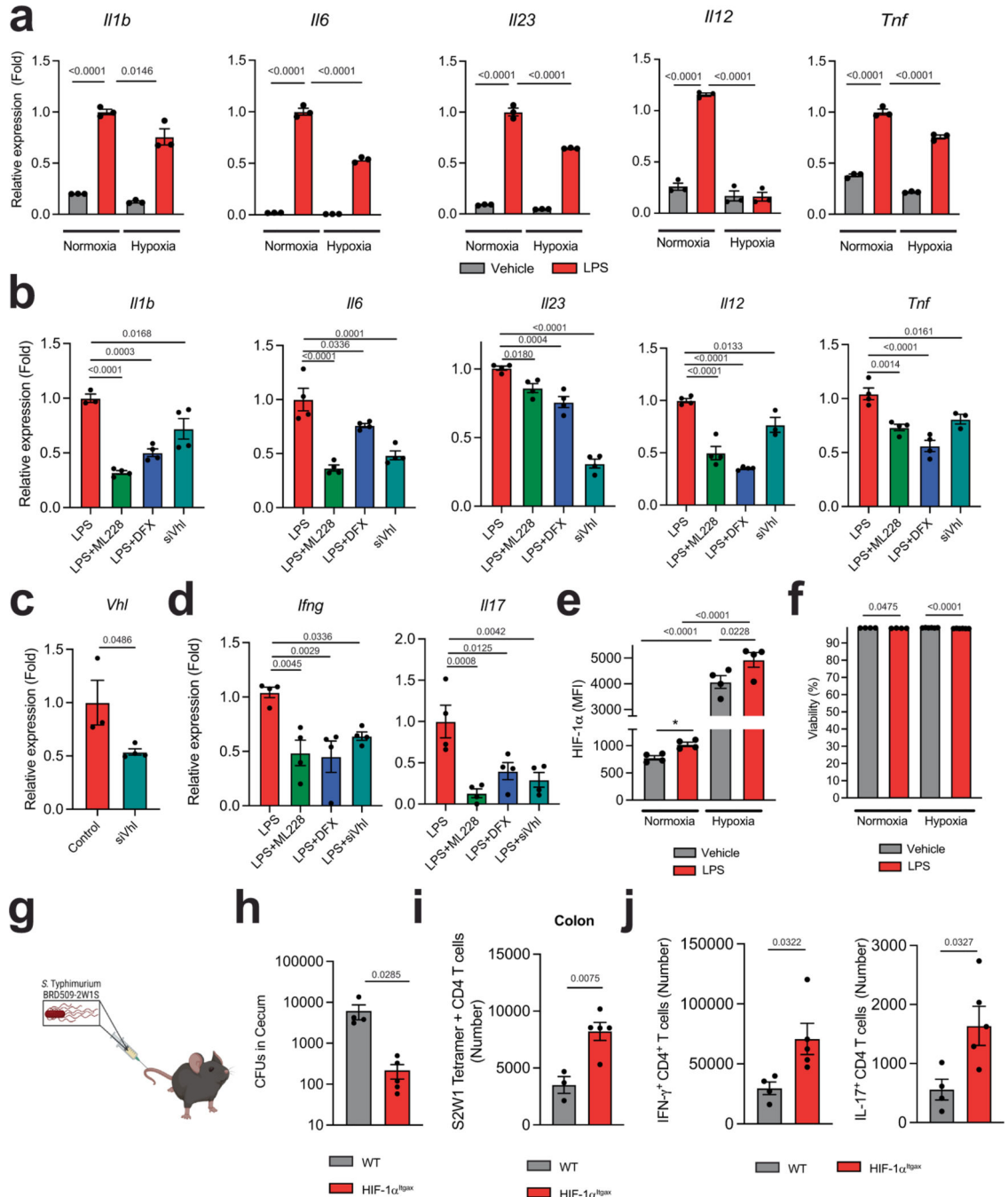
Further information on research design is available in the Nature Portfolio Reporting Summary linked to this article.

## Extended Data

Extended Data Fig. 1 | Analysis of HIF-1<sup>Itgax</sup> mice during EAE.

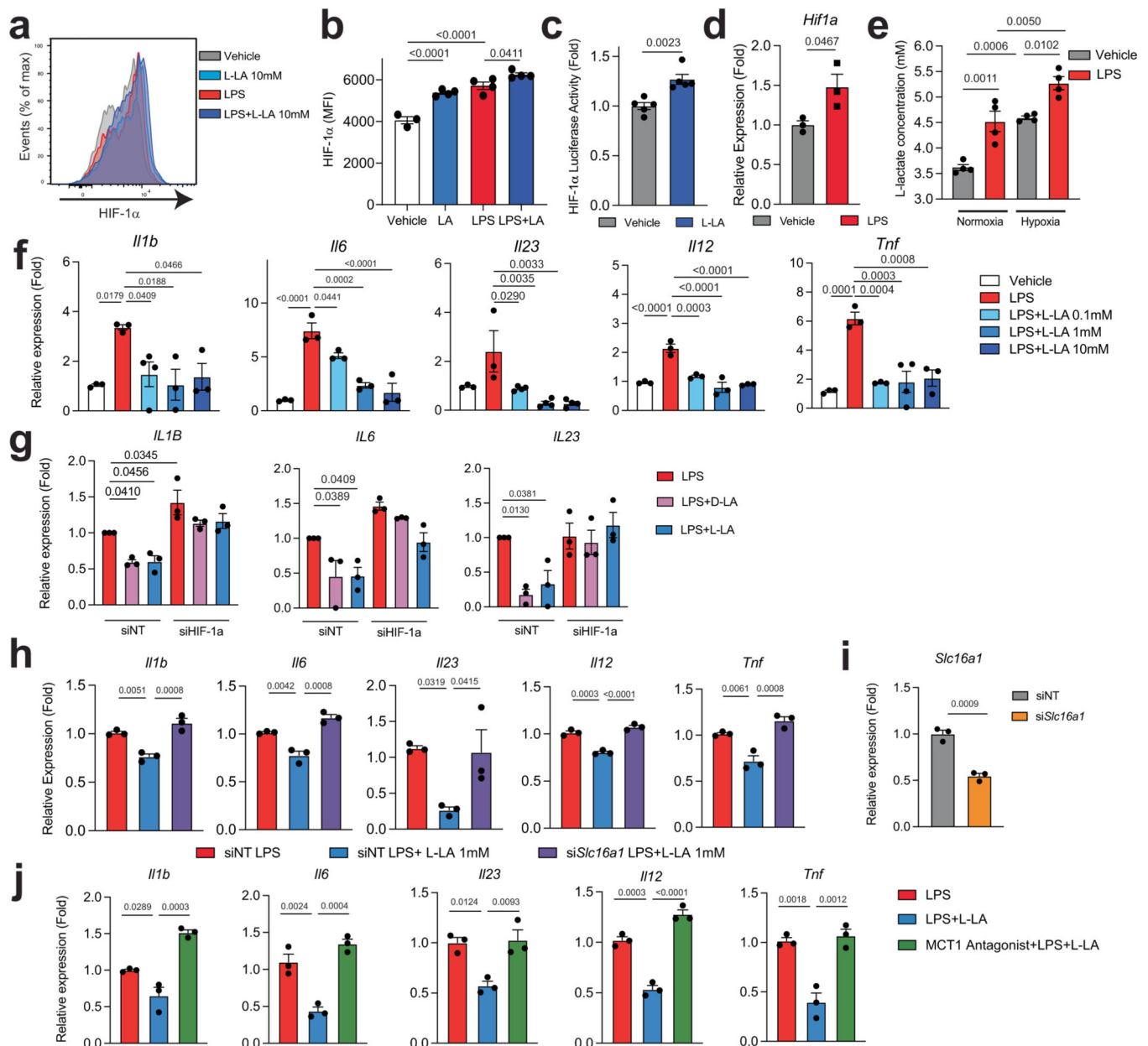
**a**, Uniform manifold approximation and projection (UMAP) displaying CNS DCs analysed by scRNA-seq during EAE. **b**, GSEA of hypoxia activation in DC subsets (cDC1, cDC2 and pDC) from scRNA-seq dataset<sup>53</sup>. **c,d**, Representative dot plot (**c**) and flow cytometry analysis (**d**) of HIF-1α expression in splenic cDC1s (CD8<sup>+</sup>CD11b<sup>-</sup>), cDC2s (CD8<sup>-</sup>CD11b<sup>-</sup>) and pDCs (B220<sup>+</sup>) 25 days after EAE induction in WT mice ( $n = 5$  mice per group). **e**, Gating strategy used to analyse CD4<sup>+</sup> T cells in the CNS of mice subjected to EAE. **f**, IFN-γ<sup>+</sup>, IFN-γ<sup>+</sup>IL-17<sup>+</sup> CD4<sup>+</sup> T cells in spleens of WT ( $n = 5$ ) and HIF-1α<sup>Itgax</sup> ( $n = 4$ ) mice subjected to EAE. **g,h**, Cytokine production (20 μg/mL MOG<sub>33-55</sub>) (**g**) and proliferative

recall response to ex vivo MOG<sub>35-55</sub> restimulation (**h**) of splenocytes isolated from mice from (**f** ( $n = 3$  for WT IFN $\gamma$ ,  $n = 4$  for HIF-1 $\alpha$ <sup>tgax</sup> IFN $\gamma$ , IL-17 and WT GM-CSF,  $n = 5$  otherwise). **i**, Absolute number of DCs in CNS from WT and HIF-1 $\alpha$ <sup>tgax</sup> mice ( $n = 5$  mice per group). **j-l**, Heat map (**j**), IPA (**k**) and GSEA analysis (**l**) of RNA-seq of DCs isolated from the CNS of WT or HIF-1 $\alpha$ <sup>tgax</sup> mice subjected to EAE. Statistical analysis was performed using unpaired Student's *t*-test for **f** and **g** and two-way ANOVA followed by Šídák's multiple comparisons test for **h**. Data shown as mean  $\pm$  s.e.m.



**Extended Data Fig. 2 |. Effects of HIF-1 $\alpha$  in DCs.**

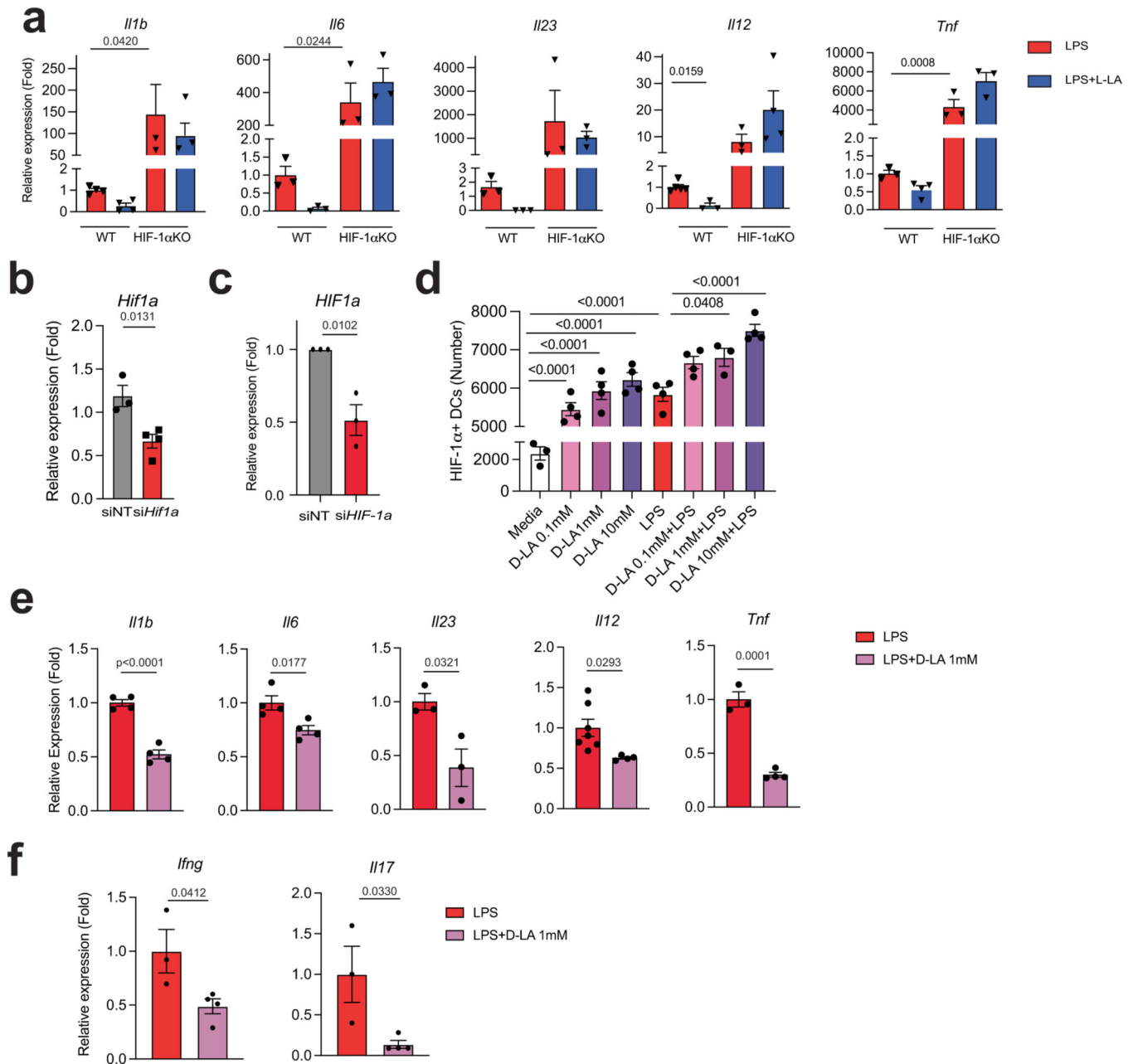
**a**, mRNA expression of shown genes in BMDCs isolated from WT mice treated with either vehicle or LPS and subjected to normoxia or hypoxia ( $n = 3$  per group) **b**, mRNA expression of shown genes in BMDCs isolated from WT mice treated with LPS and ML228, DFX, or after *Vhl* knockdown (si *Vhl*) ( $n = 3$ -for *Iil1b* after LPS, *Iil12a* and *Tnf* for siVhl,  $n = 4$  otherwise). **c**, *Vhl* expression in si *Vhl*-treated BMDCs from **b** ( $n = 3$  for siNT,  $n = 4$  for siVhl). **d**, *Iing* and *Iil17a* expression in 2D2<sup>+</sup> CD4<sup>+</sup> T cells co-cultured with WT BMDCs pre-stimulated with LPS and ML228, DFX or si *Vhl* ( $n = 4$  per group). **e,f**, HIF-1 $\alpha$  MFI (**e**) and frequency of viable cells (**f**) of BMDCs following LPS stimulation and subjected to normoxia or hypoxia ( $n = 6$  for viability after hypoxia,  $n = 4$  otherwise). **g,h**, Experimental design (**g**) and *S. typhimurium* CFU quantification (**h**) in caecum from WT ( $n = 4$ ) and HIF-1 $\alpha$ <sup>Igax</sup> ( $n = 5$ ) mice 14 days after infection. **i,j**, S2W1 Tetramer-specific (**i**) and IFN $\gamma$ <sup>+</sup> and IL-17<sup>+</sup> (**j**) CD4<sup>+</sup> T cells in colon from mice from **h**. Statistical analysis was performed using one-way ANOVA with Tukey's, Dunnett's or Šídák's post-hoc test for selected multiple comparisons for **a,b,d-f**, or unpaired Student's *t*-test for **c, h-j**. Data shown as mean  $\pm$  s.e.m.



### Extended Data Fig. 3 | Effects of HIF-1 $\alpha$ activation by L-LA on DCs

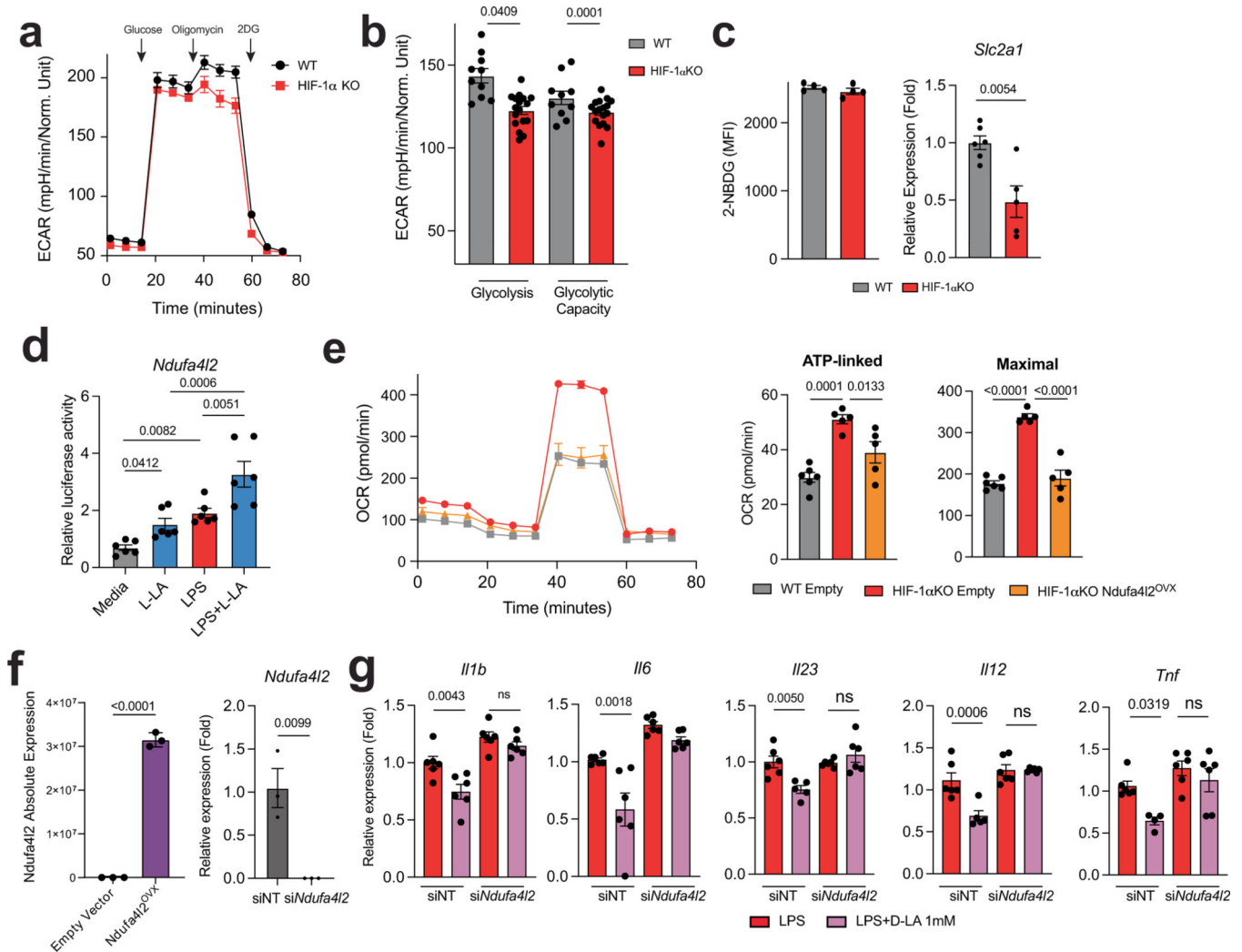
**ab**, Representative histogram (**a**) and MFI (**b**) of HIF-1 $\alpha$  expression in BMDCs isolated from WT mice and treated with vehicle, LPS, L-LA, or both LPS and L-LA ( $n = 3$  for vehicle,  $n = 4$  otherwise). **c**, HIF-1 $\alpha$  luciferase activity in BMDCs isolated from FVB.129S6-Gt(ROSA)26Sor<sup>tm2(HIF1A/luc)Kael/J</sup> mice and treated with L-LA ( $n = 5$  per group). **d**, *Hif1a* expression in BMDCs treated with vehicle or LPS ( $n = 3$  per group). **e**, L-LA production of WT mouse BMDCs treated with vehicle or LPS and subjected to normoxia or hypoxia conditions ( $n = 4$  per group). **f**, mRNA expression of shown genes in WT mouse BMDCs treated with vehicle or LPS and varying concentrations of L-LA ( $n = 4$  for *Il1b* LPS+LA 0.1mM, *Il23a* LPS+LA 0.1, 1 and 10 mM and *Tnf* LPS+LA 1mM,  $n = 4$  otherwise). **g**, mRNA expression of shown genes in human DCs after *HIF1A*

knockdown (si*HIF1A*) or control (siNT) treated with LPS and L-LA or D-LA ( $n = 3$  per group). **h-j**, mRNA expression of shown genes in WT mouse BMDCs after *Slc16a1* knockdown (si*Slc16a1*) or control (siNT) (**h,i**) or treatment with the MCT1-antagonist AZD3965 (**j**) treated LPS and L-LA ( $n = 3$  per group). Statistical analysis was performed using one-way ANOVA with Tukey's, Šidák's or Holm-Šidák's post-hoc test for selected multiple comparisons for **b,e-h,j**, or unpaired Student's *t*-test for **c,d,i**. Data shown as mean  $\pm$  s.e.m.



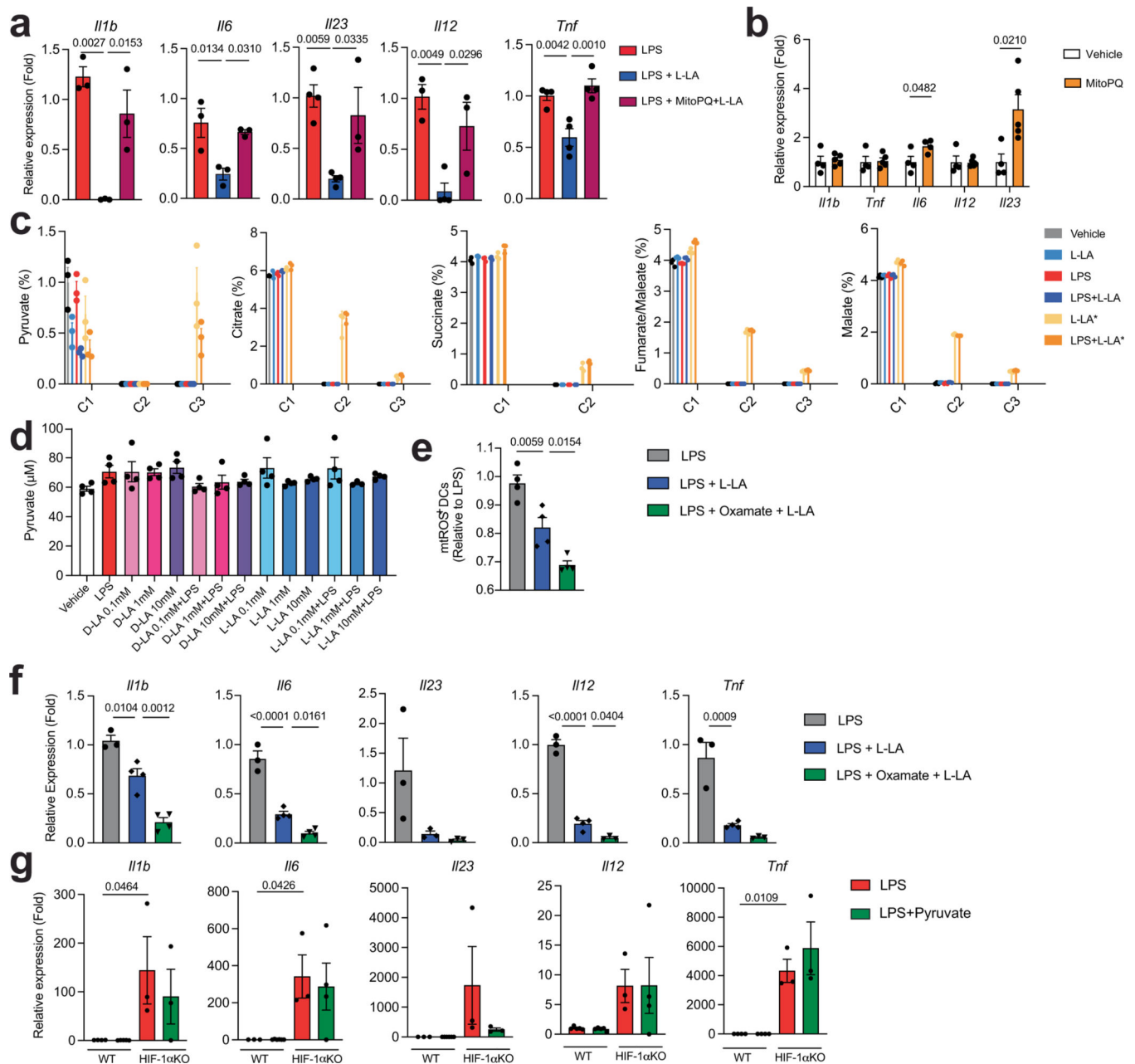
Extended Data Fig. 4 | Effects of HIF-1 $\alpha$  activation by D-LA on DCs.

**a**, mRNA expression of shown genes in splenic DCs isolated from WT or HIF-1 $\alpha$ <sup>Itgax</sup> mice stimulated with LPS or LPS and L-LA ( $n = 3-4$  per group). **b,c**, mRNA expression of *Hif1a* (**b**) or *HIF1A* (**c**) after knockdown in mouse BMDCs (**b**) and human DCs (**c**) ( $n = 4$  for siHif1 in BMDCs,  $n = 3$  otherwise). **d**, Absolute numbers of HIF-1 $\alpha$ <sup>+</sup> DCs following treatment with D-LA or LPS with D-LA ( $n = 3$  for media and LPS+D-LA 1 mM,  $n = 4$  otherwise). **e**, mRNA expression of shown genes in splenic DCs from WT mice after LPS treatment with or without D-LA (1mM) treatment for 6h ( $n = 7$  for *Il23a* in LPS treatment,  $n = 3$  for *Il23a* in LPS and LPS+D-LA and *Tnf* in LPS,  $n = 4$  otherwise). **f**, *Ifng* and *Il17a* expression in 2D2<sup>+</sup> CD4<sup>+</sup> T cells co-cultured DCs pre-treated with LPS or LPS and D-LA (1mM) ( $n = 3$  for LPS-treated cells,  $n = 4$  otherwise). Statistical analysis was performed using one-way ANOVA with Tukey's, Šídák's or Dunnett's post-hoc test for selected multiple comparisons for **a** and **d**, or unpaired Student's *t*-test for **b,c,e,f**. Data shown as mean  $\pm$  s.e.m.



Extended Data Fig. 5 | Effects of HIF-1 $\alpha$  on DC metabolism.

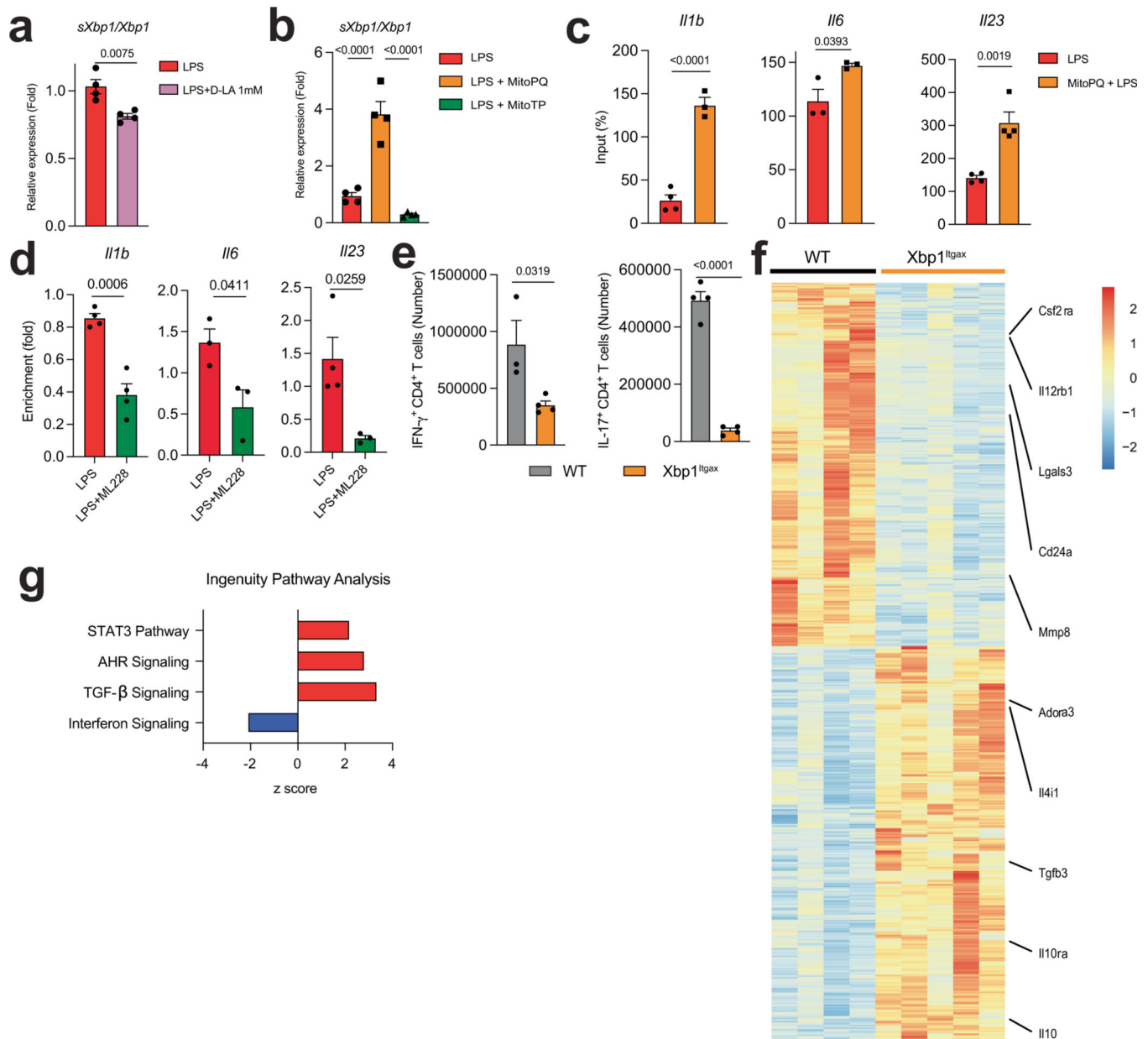
**a**, ECAR in BMDCs isolated from WT or HIF-1 $\alpha$ <sup>I<sup>tgax</sup></sup> mice after glucose, oligomycin and 2-DG treatment ( $n = 10$  WT and 20 HIF-1 $\alpha$  KO replicate wells). **b**, Glycolysis and glycolytic capacity in WT and HIF-1 $\alpha$ <sup>I<sup>tgax</sup></sup> BMDCs from **a** ( $n = 10$  WT and 17 HIF-1 $\alpha$  KO replicate wells). **c**, 2-NBDG uptake and *Slc2a1* expression in BMDCs isolated from WT and HIF-1 $\alpha$ <sup>I<sup>tgax</sup></sup> mice and stimulated with LPS ( $n = 4-6$  per group). **d**, Transactivation of *Ndufa412* promoter in *Ndufa412*-luciferase transfected DC2.4 cells treated with L-LA or LPS for 24 h ( $n = 3$  per group). **e**, OCR in BMDCs isolated from WT or HIF-1 $\alpha$ <sup>I<sup>tgax</sup></sup> mice and transfected with either an empty or *Ndufa412*-overexpression plasmid ( $n = 6$  for WT,  $n = 5$  otherwise). **f**, *Ndufa412* expression after transfection with *Ndufa412*-overexpression plasmid or silencing with siRNA ( $n = 3$  per group). **g**, mRNA expression of shown genes in WT mouse BMDCs after *Ndufa412* knockdown (si*Ndufa412*) or controls (siNT) stimulated with LPS and treated with or without D-LA for 6 h ( $n = 5$  for *Il23a* siNT LPS + D-LA,  $n = 6$  otherwise). Statistical analysis was performed using unpaired Student's *t*-test for **b,c,f** and one-way ANOVA with Šídák's or Holm-Šídák's post-hoc test for selected multiple comparisons for **d,e,g**. Data shown as mean  $\pm$  s.e.m.



### Extended Data Fig. 6 | Incorporation of L-LA into TCA intermediates.

**a**, mRNA expression of shown genes in BMDCs isolated from WT mice and stimulated with LPS and mitoPQ or L-LA for 6 h ( $n = 3-4$  per group). **b**, mRNA expression of shown genes in BMDCs isolated from WT mice and treated with mitoPQ for 6 h ( $n = 4-5$  per group). **c**, <sup>13</sup>C incorporation into TCA intermediates in BMDCs isolated from WT mice and treated with uniformly labelled <sup>13</sup>C-lactate (L-LA\*), L-LA or LPS for 1 h ( $n = 3$  per group). **d**, Pyruvate intracellular levels in WT BMDCs after treatment with LPS, L-LA or D-LA for 1 h ( $n = 4$  per group). **e,f**, mtROS production (**e**) and mRNA expression of shown genes (**f**) in WT BMDCs pre-treated with LDH-inhibitor oxamate, L-LA or LPS ( $n = 3-4$  per group). **g**, mRNA expression of shown genes in splenic DCs isolated from WT or HIF-1α<sup>Itgax</sup> mice

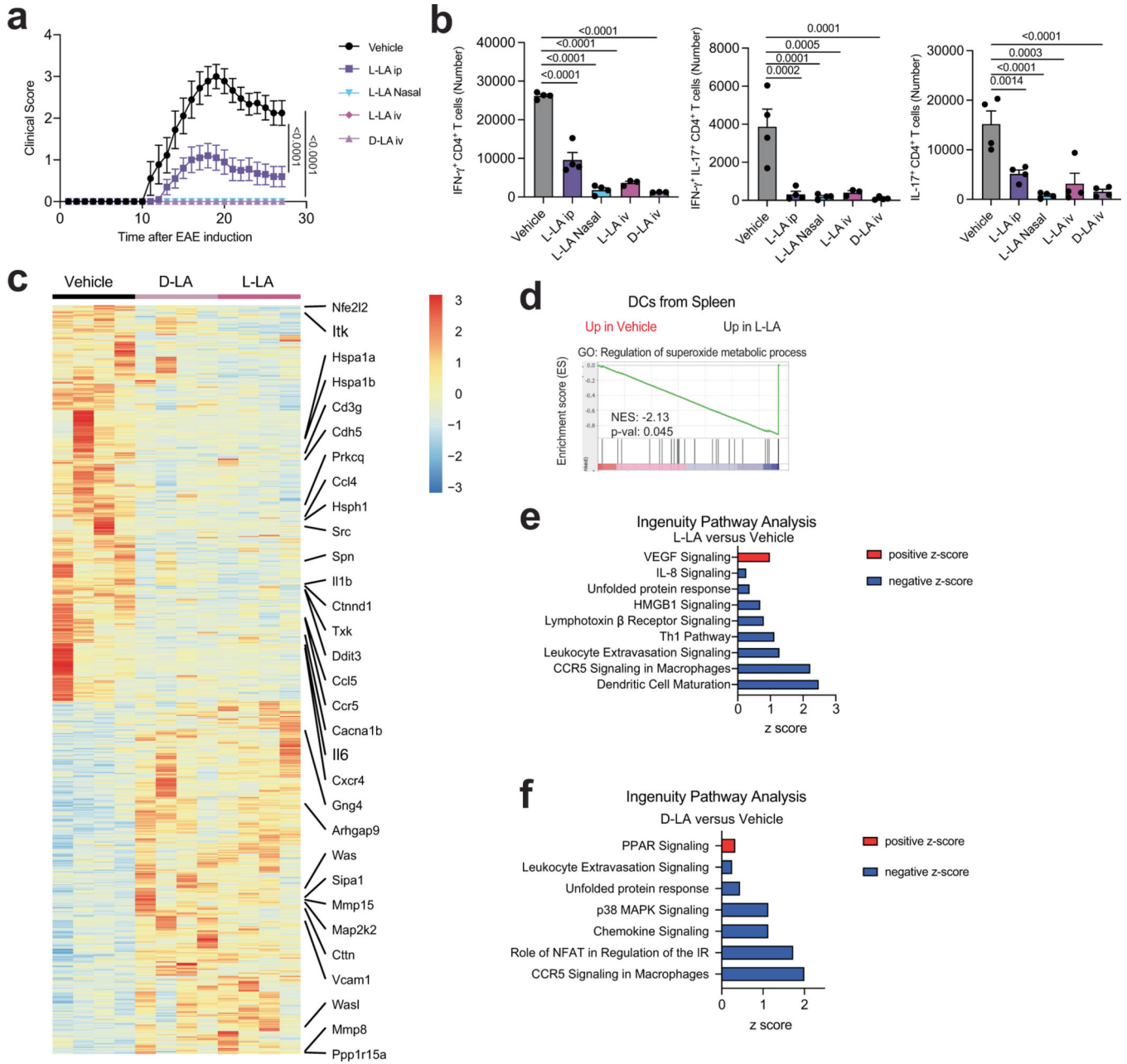
then treated with LPS or pyruvate for 6 h ( $n = 3-4$  per group). Statistical analysis was performed using one-way ANOVA with Tukey's, Šídák's or Dunnett's post-hoc test for selected multiple comparisons for **a,e-g** and unpaired Student's *t*-test for **b**. Data shown as mean  $\pm$  s.e.m.



**Extended Data Fig. 7 | Control of DCs by XBP1.**

**a,b**, *sXbp1/Xbp1* mRNA ratio in BMDCs isolated from WT mice and treated with LPS or LPS+D-LA (**a**) and LPS, mitoPQ or mitoTempo (MitoTP) (**b**) for 6 h ( $n = 4$  per group). **c,d**, XBP1 recruitment to the *Il1b*, *Il6* and *Il23a* promoters in WT BMDCs treated with LPS and mitoPQ (**c**) or LPS and ML228 (**d**) for 6h. **e**, Total numbers of IFN $\gamma^+$  and IL-17 $^+$  CD4 $^+$  splenic T cells in WT ( $n = 3-4$ ) and Xbp1<sup>Ilgax</sup> ( $n = 4$ ) mice 30 days after EAE induction.

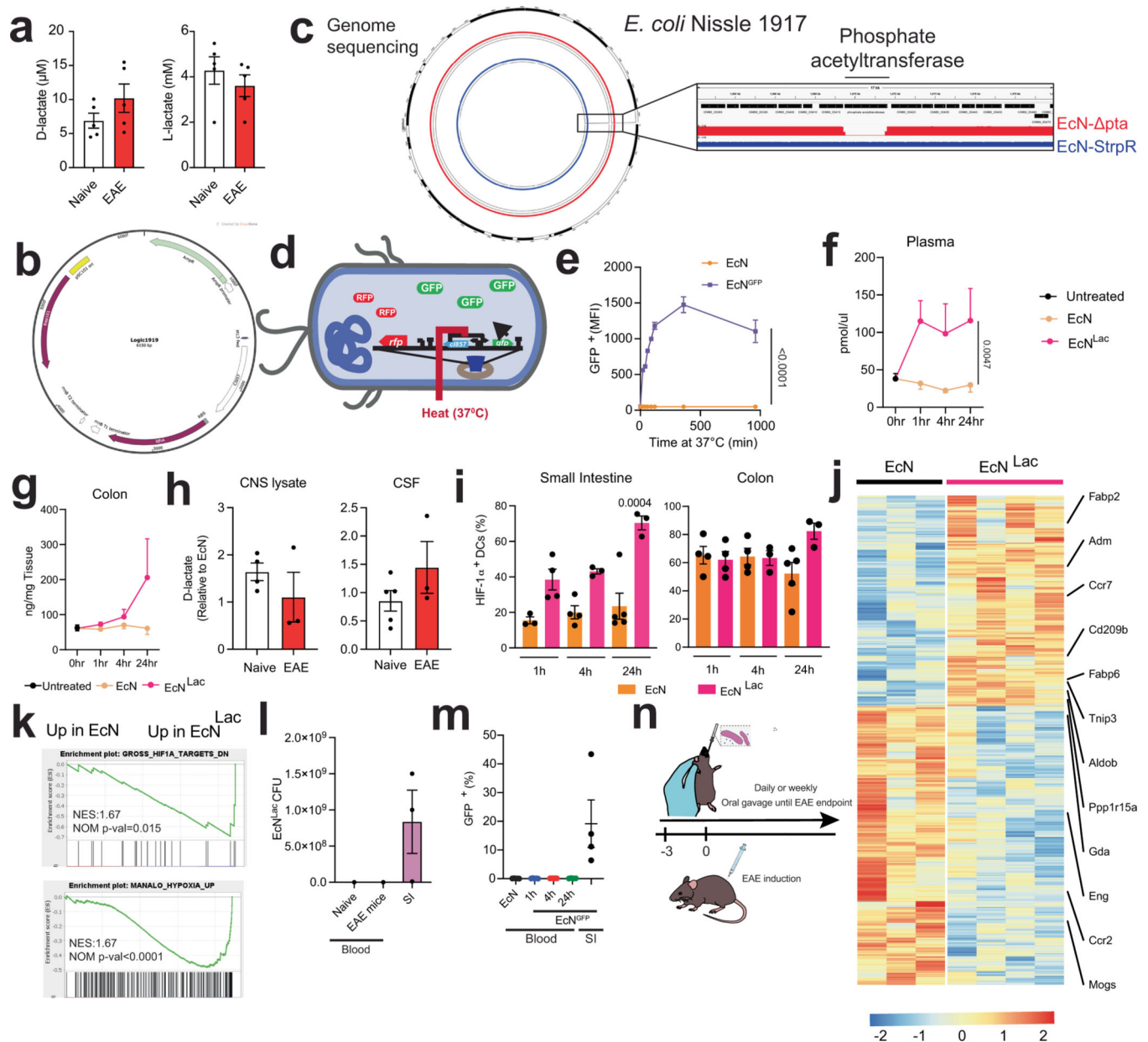
**f,g**, Heat map (**f**) and IPA (**g**) in CNS DCs from WT ( $n = 4$ ) and  $Xbp1^{Itgax}$  ( $n = 5$ ) mice 30 days after EAE induction. Statistical analysis was performed using unpaired Student's  $t$ -test for **a,c-e** and one-way ANOVA with Šídák's post-hoc test for selected multiple comparisons for **b**. Data shown as mean  $\pm$  s.e.m.



**Extended Data Fig. 8 | Effect of lactate on EAE.**

**a**, EAE development of mice after vehicle injection ( $n = 9$ ), intraperitoneal (ip) ( $n = 10$ ), nasal, or intravenous (iv) ( $n = 5$  per group) L-LA or D-LA administration. **b**,  $IFN\gamma^+$ ,  $IFN\gamma^+IL-17^+$  and  $IL-17^+ CD4^+$  T cells in CNS isolated from mice from **a** 28 days after EAE induction ( $n = 3-4$  per group). **c-f**, Heat map (**c**), GSEA (**d**) and IPA (**e,f**) analysis of

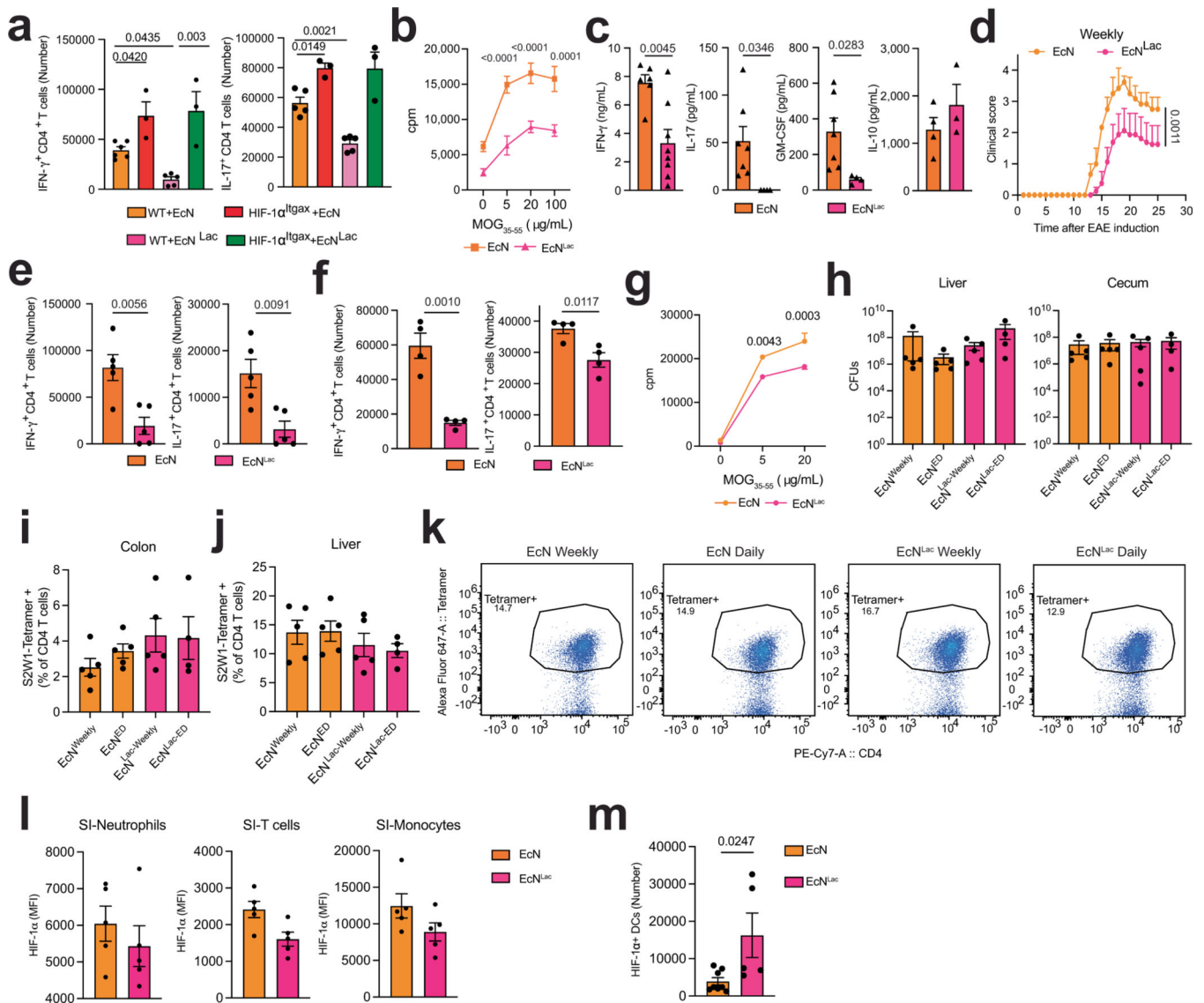
RNA-seq of splenic DCs isolated from mice treated with vehicle, L-LA (e) and D-LA (f) 28 days after EAE induction. Statistical analysis was performed using two-way ANOVA for a and one-way ANOVA with Dunnett's post-hoc test for selected multiple comparisons for b. Data shown as mean  $\pm$  s.e.m.



### Extended Data Fig. 9 | EcN<sup>Lac</sup> characterization.

**a**, L-LA and D-LA concentration in plasma taken from naive and peak EAE WT mice ( $n = 5$  per group). **b**, Schematic depicting the genome sequencing of EcN<sup>Lac</sup> and parental EcN strains. **c**, Schematic for the plasmid used to induce *ldhA* expression in the EcN<sup>Lac</sup> engineered strain. **d**, EcN<sup>GFP</sup> reporter strain. **e**, GFP expression in EcN<sup>GFP</sup> after activation at 37°C. **f, g**, D-LA concentration in plasma (**f**) and colon tissue (**g**) after EcN<sup>Lac</sup> or EcN

administration ( $n = 5-9$  mice per group). **h**, D-LA concentration in CSF and CNS lysate from naive ( $n = 4-5$ ) and EAE ( $n = 3$ ) WT mice after EcN<sup>Lac</sup> administration, shown relative to D-LA concentration levels in EcN-treated mice. **i**, Percentage of HIF-1 $\alpha$ <sup>+</sup> DCs out of total DCs isolated from small intestine and colon tissue from EcN ( $n = 3-5$ ) or EcN<sup>Lac</sup> ( $n = 3-4$ ) treated mice. **j,k**, Heat map (**j**) and GSEA (**k**) analysis of RNA-seq of DCs isolated from the small intestine of EcN ( $n = 3$ ) or EcN<sup>Lac</sup> ( $n = 4$ ) treated mice. **l,m**, EcN<sup>Lac</sup> CFUs in blood isolated from naive and peak EAE mice treated with EcN<sup>Lac</sup> daily for a week (**l**) and EcN<sup>GFP</sup> in blood 1, 4 and 24 h after oral gavage (**m**). Small intestine CFU levels are shown as positive controls ( $n = 4-5$  per group). **n**, Experimental design to assess the effect of EcN<sup>Lac</sup> daily or weekly administration on EAE disease course. Statistical analysis was performed using two-way ANOVA with Šídák's post-hoc test for **e,f**, and one-way ANOVA with Dunnett's post-hoc test for selected multiple comparisons for **i**. Data shown as mean  $\pm$  s.e.m.



**Extended Data Fig. 10 | Effects of EcN<sup>Lac</sup> on EAE and *S. typhimurium* infection.**

**a**, Splenic IFN $\gamma^+$  and IL-17<sup>+</sup>CD4<sup>+</sup> T cells isolated 20 days after EAE induction from WT mice treated with EcN ( $n = 5-6$ ) or EcN<sup>Lac</sup> ( $n = 5$ ) and HIF-1 $\alpha^{\text{I}g\alpha\text{x}}$  mice treated with EcN ( $n = 3$ ) or EcN<sup>Lac</sup> ( $n = 3$ ). **b,c**, Proliferative recall response to ex vivo MOG<sub>35-55</sub> restimulation (**b**) and cytokine production (20  $\mu\text{g ml}^{-1}$  MOG<sub>33-55</sub>) (**c**) of splenocytes isolated 20 days after EAE induction from WT mice dosed daily with EcN ( $n = 4-8$ ) or EcN<sup>Lac</sup> ( $n = 3-8$ ). **d-g**, EAE development (**d**), IFN $\gamma^+$  and IL-17<sup>+</sup>CD4<sup>+</sup> T cells in CNS (**e**) and spleen (**f**), and splenocyte proliferation recall response (**g**) to ex vivo MOG<sub>35-55</sub> restimulation of WT mice treated weekly with EcN ( $n = 4-5$ ) or EcN<sup>Lac</sup> ( $n = 4-5$ ). **h**, CFUs in liver and caecum from WT mice infected with *S. typhimurium* after daily or weekly administration of EcN ( $n = 5$ ) or EcN<sup>Lac</sup> ( $n = 4-5$ ). **i-k**, Percentage of S2W1 tetramer<sup>+</sup> out of total CD4 T cells in colon (**i**), and liver (**j**) and representative S2W1 tetramer staining of CD4 T cells in liver (**k**) in mice from **h**. **l,m**, HIF-1 $\alpha$  MFI in neutrophils, monocytes and T cells (**l**), and number of HIF-1 $\alpha^+$  DCs (**m**) in small intestine as a result of daily EcN ( $n = 5-8$ ) or EcN<sup>Lac</sup> ( $n = 5$ ) treatment of WT mice for one week. Statistical analysis was performed using one-way ANOVA with Dunnett's post-hoc test for selected multiple comparisons for **a**, two-way ANOVA followed by Šídák's multiple comparisons test for **b,d,g** and unpaired Student's *t*-test for **c,e,f,m**. Data shown as mean  $\pm$  s.e.m.

**Acknowledgements**

This work was supported by grants NS102807, ES02530, ES029136 and AI126880 from the National Institutes of Health (NIH); RG4111A1 and JF2161-A-5 from the National Multiple Sclerosis Society; RSG-14-198-01-LIB from the American Cancer Society; and PA-160408459 from the International Progressive MS Alliance (to F.J.Q.). C.M.P. was supported by a fellowship from FAPESP BEPE (2019/13731-0) and by the Herbert R. & Jeanne C. Mayer Foundation; G.F.L. received support from a grant from the Swedish Research Council (2021-06735); C.G.-V. was supported by an Alfonso Martin Escudero Foundation postdoctoral fellowship and by a postdoctoral fellowship (ALTF 610-2017) from the European Molecular Biology Organization; C.-C.C. received support from a postdoctoral research abroad program (104-2917-I-564-024) from the Ministry of Science and Technology, Taiwan; C.M.R.-G. was supported by a predoctoral F.P.U. fellowship from the Ministry of Economy and Competitiveness and by the European Union FEDERER program; M.A.W. was supported by NIH (1K99NS114111, F32NS101790 and T32CA207201), the Program in Interdisciplinary Neuroscience and the Women's Brain Initiative at Brigham and Women's Hospital; T.I. was supported by an EMBO postdoctoral fellowship (ALTF: 1009-2021) and H.-G.L. was supported by the Basic Science Research Program through the National Research Foundation of Korea (NRF) funded by the Ministry of Education (2021R1A6A3A14039088). We thank L. Glimcher and J. R. Cubillos Ruiz for sharing *Itgax<sup>Cre</sup>Xbp1<sup>fllox</sup>* mice; S. McSorley for providing the *S. typhimurium* strain; H. Xu and M. Lehtinen for providing training on CSF extraction; all members of the F.J.Q. laboratory for advice and discussions; R. Krishnan for technical assistance with flow cytometry studies; and the NeuroTechnology Studio at Brigham and Women's Hospital for providing access to Seahorse instruments.

**Data availability**

All raw and processed deep -sequencing data have been deposited at the Gene Expression Omnibus (GEO) with accession code GSE188504.

**References**

1. Anderson DA III, Dutertre CA, Ginhoux F. & Murphy KM Genetic models of human and mouse dendritic cell development and function. *Nat. Rev. Immunol* 21, 101–115 (2021). [PubMed: 32908299]
2. Cabeza-Cabrerizo M, Cardoso A, Minutti CM, Pereira da Costa M. & Reis ESC Dendritic cells revisited. *Annu. Rev. Immunol* 39, 131–166 (2021). [PubMed: 33481643]

3. Nasser J. et al. . Genome-wide enhancer maps link risk variants to disease genes. *Nature* 593, 238–243 (2021). [PubMed: 33828297]
4. Saevarsdottir S. et al. *FLT3* stop mutation increases FLT3 ligand level and risk of autoimmune thyroid disease. *Nature* 584, 619–623 (2020). [PubMed: 32581359]
5. Dixon KO et al. TIM-3 restrains anti-tumour immunity by regulating inflammasome activation. *Nature* 595, 101–106 (2021). [PubMed: 34108686]
6. Ferris ST et al. cDC1 prime and are licensed by CD4<sup>+</sup> T cells to induce anti-tumour immunity. *Nature* 584, 624–629 (2020). [PubMed: 32788723]
7. Buck MD, Sowell RT, Kaech SM & Pearce EL Metabolic instruction of immunity. *Cell* 169, 570–586 (2017). [PubMed: 28475890]
8. Du X. et al. Hippo/Mst signalling couples metabolic state and immune function of CD8 $\alpha$ <sup>+</sup> dendritic cells. *Nature* 558, 141–145 (2018). [PubMed: 29849151]
9. Campbell C. et al. Bacterial metabolism of bile acids promotes generation of peripheral regulatory T cells. *Nature* 581, 475–479 (2020). [PubMed: 32461639]
10. Suez J, Zmora N, Segal E. & Elinav E. The pros, cons, and many unknowns of probiotics. *Nat. Med* 25, 716–729 (2019). [PubMed: 31061539]
11. Buffington SA et al. Dissecting the contribution of host genetics and the microbiome in complex behaviors. *Cell* 184, 1740–1756 (2021). [PubMed: 33705688]
12. Canale FP et al. Metabolic modulation of tumours with engineered bacteria for immunotherapy. *Nature* 598, 662–666 (2021). [PubMed: 34616044]
13. Scott BM et al. Self-tunable engineered yeast probiotics for the treatment of inflammatory bowel disease. *Nat. Med* 27, 1212–1222 (2021). [PubMed: 34183837]
14. Colegio OR et al. Functional polarization of tumour-associated macrophages by tumour-derived lactic acid. *Nature* 513, 559–563 (2014). [PubMed: 25043024]
15. Benoun JM et al. Optimal protection against *Salmonella* infection requires noncirculating memory. *Proc. Natl Acad. Sci. USA* 115, 10416–10421 (2018). [PubMed: 30254173]
16. Tannahill GM et al. Succinate is an inflammatory signal that induces IL-1 $\beta$  through HIF-1 $\alpha$ . *Nature* 496, 238–242 (2013). [PubMed: 23535595]
17. Safran M. et al. Mouse model for noninvasive imaging of HIF prolyl hydroxylase activity: assessment of an oral agent that stimulates erythropoietin production. *Proc. Natl Acad. Sci. USA* 103, 105–110 (2006). [PubMed: 16373502]
18. Bosshart PD, Kalbermatter D, Bonetti S. & Fotiadis D. Mechanistic basis of l-lactate transport in the SLC16 solute carrier family. *Nat. Commun* 10, 2649 (2019). [PubMed: 31201333]
19. Brown TP et al. The lactate receptor GPR81 promotes breast cancer growth via a paracrine mechanism involving antigen-presenting cells in the tumor microenvironment. *Oncogene* 39, 3292–3304 (2020). [PubMed: 32071396]
20. Levitt MD & Levitt DG Quantitative evaluation of d-lactate pathophysiology: new insights into the mechanisms involved and the many areas in need of further investigation. *Clin. Exp. Gastroenterol* 13, 321–337 (2020). [PubMed: 32982363]
21. Colgan SP, Furuta GT & Taylor CT Hypoxia and innate immunity: keeping up with the HIFsters. *Annu. Rev. Immunol* 38, 341–363 (2020). [PubMed: 31961750]
22. Tello D. et al. Induction of the mitochondrial NDUFA4L2 protein by HIF-1 $\alpha$  decreases oxygen consumption by inhibiting complex I activity. *Cell Metab.* 14, 768–779 (2011). [PubMed: 22100406]
23. Mogilenko DA et al. Metabolic and innate immune cues merge into a specific inflammatory response via the UPR. *Cell* 177, 1201–1216 (2019). [PubMed: 31031005]
24. Martinez-Reyes I. & Chandel NS Mitochondrial TCA cycle metabolites control physiology and disease. *Nat. Commun* 11, 102 (2020). [PubMed: 31900386]
25. Martinon F, Chen X, Lee AH & Glimcher LH TLR activation of the transcription factor XBP1 regulates innate immune responses in macrophages. *Nat. Immunol* 11, 411–418 (2010). [PubMed: 20351694]
26. Cubillos-Ruiz JR et al. ER stress sensor XBP1 controls anti-tumor immunity by disrupting dendritic cell homeostasis. *Cell* 161, 1527–1538 (2015). [PubMed: 26073941]

27. Puurunen MK et al. Safety and pharmacodynamics of an engineered *E. coli* Nissle for the treatment of phenylketonuria: a first-in-human phase 1/2a study. *Nat. Metab* 3, 1125–1132 (2021). [PubMed: 34294923]
28. Kurtz CB et al. An engineered *E. coli* Nissle improves hyperammonemia and survival in mice and shows dose-dependent exposure in healthy humans. *Sci. Transl. Med* 11, eaau7975 (2019).
29. Castano-Cerezo S. et al. An insight into the role of phosphotransacetylase (pta) and the acetate/acetyl-CoA node in *Escherichia coli*. *Microb. Cell Fact* 8, 54 (2009). [PubMed: 19852855]
30. Enjalbert B, Millard P, Dinclaux M, Portais JC & Letisse F. Acetate fluxes in *Escherichia coli* are determined by the thermodynamic control of the Pta–AckA pathway. *Sci. Rep* 7, 42135 (2017). [PubMed: 28186174]
31. Berer K. et al. Commensal microbiota and myelin autoantigen cooperate to trigger autoimmune demyelination. *Nature* 479, 538–541 (2011). [PubMed: 22031325]
32. Hiltensperger M. et al. Skin and gut imprinted helper T cell subsets exhibit distinct functional phenotypes in central nervous system autoimmunity. *Nat. Immunol* 22, 880–892 (2021). [PubMed: 34099917]
33. Schnell A. et al. Stem-like intestinal Th17 cells give rise to pathogenic effector T cells during autoimmunity. *Cell* 184, 6281–6298 (2021). [PubMed: 34875227]
34. Tomura M. et al. Monitoring cellular movement in vivo with photoconvertible fluorescence protein “Kaede” transgenic mice. *Proc. Natl Acad. Sci. USA* 105, 10871–10876 (2008). [PubMed: 18663225]
35. D’Ignazio L, Bandarra D. & Rocha S. NF- $\kappa$ B and HIF crosstalk in immune responses. *FEBS J.* 283, 413–424 (2016). [PubMed: 26513405]
36. O’Neill LA, Kishton RJ & Rathmell J. A guide to immunometabolism for immunologists. *Nat. Rev. Immunol* 16, 553–565 (2016). [PubMed: 27396447]
37. Aste-Amezaga M, Ma X, Sartori A. & Trinchieri G. Molecular mechanisms of the induction of IL-12 and its inhibition by IL-10. *J. Immunol* 160, 5936–5944 (1998). [PubMed: 9637507]
38. Mascanfroni ID et al. IL-27 acts on DCs to suppress the T cell response and autoimmunity by inducing expression of the immunoregulatory molecule CD39. *Nat. Immunol* 14, 1054–1063 (2013). [PubMed: 23995234]
39. Lawless SJ et al. Glucose represses dendritic cell-induced T cell responses. *Nat. Commun* 8, 15620 (2017). [PubMed: 28555668]
40. Zhang D. et al. Metabolic regulation of gene expression by histone lactylation. *Nature* 574, 575–580 (2019). [PubMed: 31645732]
41. Cheng SC et al. mTOR- and HIF-1 $\alpha$ -mediated aerobic glycolysis as metabolic basis for trained immunity. *Science* 345, 1250684 (2014). [PubMed: 25258083]
42. Watson MJ et al. Metabolic support of tumour-infiltrating regulatory T cells by lactic acid. *Nature* 591, 645–651 (2021). [PubMed: 33589820]
43. Sanmarco LM et al. Identification of environmental factors that promote intestinal inflammation. *Nature* 611, 801–809 (2022). [PubMed: 36266581]
44. Schiering C. et al. Feedback control of AHR signalling regulates intestinal immunity. *Nature* 542, 242–245 (2017). [PubMed: 28146477]
45. Opitz CA et al. An endogenous tumour-promoting ligand of the human aryl hydrocarbon receptor. *Nature* 478, 197–203 (2011). [PubMed: 21976023]
46. Takenaka MC et al. Control of tumor-associated macrophages and T cells in glioblastoma via AHR and CD39. *Nat. Neurosci* 22, 729–740 (2019). [PubMed: 30962630]
47. Rothhammer V. & Quintana FJ. The aryl hydrocarbon receptor: an environmental sensor integrating immune responses in health and disease. *Nat. Rev. Immunol* 19, 184–197 (2019). [PubMed: 30718831]
48. Mascanfroni ID et al. Metabolic control of type 1 regulatory T cell differentiation by AHR and HIF1- $\alpha$ . *Nat. Med* 21, 638–646 (2015). [PubMed: 26005855]
49. Kenison JE et al. Tolerogenic nanoparticles suppress central nervous system inflammation. *Proc. Natl Acad. Sci. USA* 117, 32017–32028 (2020). [PubMed: 33239445]

50. Krienke C. et al. A noninflammatory mRNA vaccine for treatment of experimental autoimmune encephalomyelitis. *Science* 371, 145–153 (2021). [PubMed: 33414215]
51. Bettelli E. et al. Myelin oligodendrocyte glycoprotein-specific T cell receptor transgenic mice develop spontaneous autoimmune optic neuritis. *J. Exp. Med* 197, 1073–1081 (2003). [PubMed: 12732654]
52. Sanmarco LM et al. Gut-licensed IFN $\gamma$ <sup>+</sup> NK cells drive LAMP1<sup>+</sup>TRAIL<sup>+</sup> anti-inflammatory astrocytes. *Nature* 590, 473–479 (2021). [PubMed: 33408417]
53. Wheeler MA et al. MAFG-driven astrocytes promote CNS inflammation. *Nature* 578, 593–599 (2020). [PubMed: 32051591]
54. Eberhardt N. et al. . Deficiency of CD73 activity promotes protective cardiac immunity against *Trypanosoma cruzi* infection but permissive environment in visceral adipose tissue. *Biochim. Biophys. Acta Mol. Basis Dis* 1866, 165592 (2020). [PubMed: 31678157]
55. Wheeler MA et al. Environmental control of astrocyte pathogenic activities in CNS inflammation. *Cell* 176, 581–596 (2019). [PubMed: 30661753]
56. Leventhal DS et al. Immunotherapy with engineered bacteria by targeting the STING pathway for anti-tumor immunity. *Nat. Commun* 11, 2739 (2020). [PubMed: 32483165]
57. Trombetta JJ et al. Preparation of single-cell RNA-seq libraries for next generation sequencing. *Curr. Protoc. Mol. Biol* 107, 4.22.1–4.22.17 (2014).
58. Bray NL, Pimentel H, Melsted P. & Pachter L. Near-optimal probabilistic RNA-seq quantification. *Nat. Biotechnol* 34, 525–527 (2016). [PubMed: 27043002]
59. Patro R, Duggal G, Love MI, Irizarry RA & Kingsford C. Salmon provides fast and bias-aware quantification of transcript expression. *Nat. Methods* 14, 417–419 (2017). [PubMed: 28263959]
60. Zhu A, Ibrahim JG & Love MI Heavy-tailed prior distributions for sequence count data: removing the noise and preserving large differences. *Bioinformatics* 35, 2084–2092 (2019). [PubMed: 30395178]
61. Subramanian A. et al. Gene set enrichment analysis: a knowledge-based approach for interpreting genome-wide expression profiles. *Proc. Natl Acad. Sci. USA* 102, 15545–15550 (2005). [PubMed: 16199517]
62. Mootha VK et al. PGC-1 $\alpha$ -responsive genes involved in oxidative phosphorylation are coordinately downregulated in human diabetes. *Nat. Genet* 34, 267–273 (2003). [PubMed: 12808457]
63. Illouz T, Madar R, Hirsh T, Biragyn A. & Okun E. Induction of an effective anti-Amyloid- $\beta$  humoral response in aged mice. *Vaccine* 39, 4817–4829 (2021). [PubMed: 34294479]
64. Illouz T. et al. Maternal antibodies facilitate Amyloid- $\beta$  clearance by activating Fc-receptor-Syk-mediated phagocytosis. *Commun. Biol* 4, 329 (2021). [PubMed: 33712740]
65. Haralick RM & Shapiro LG in *Computer and Robot Vision Vol. 1* (eds Haralick RM & Shapiro LG) 28–48 (Addison-Wesley, 1992).
66. Motulsky HJ, & Brown RE Detecting outliers when fitting data with nonlinear regression—a new method based on robust nonlinear regression and the false discovery rate. *BMC Bioinformatics* 7, 123 (2006). [PubMed: 16526949]

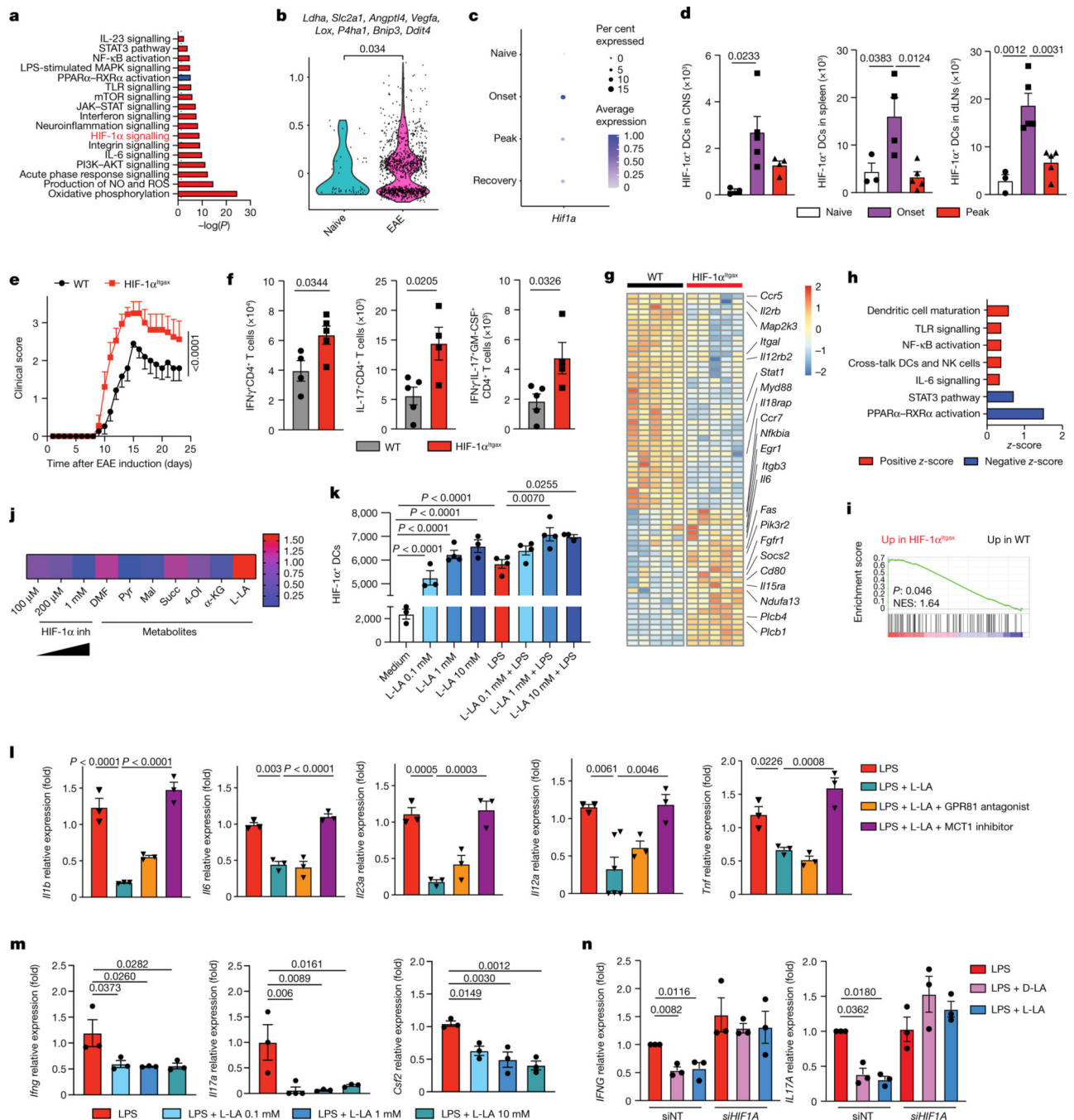


**Fig. 1 | Activation of HIF-1 $\alpha$  by lactate inhibits the pro-inflammatory activities of DCs.**

**a-c**, Ingenuity pathway analysis (IPA) (**a**), hypoxia score (**b**) and *Hif1a* expression (**c**) in total DCs from the CNS of EAE mice. **d**, Expression of HIF-1 $\alpha$  in DCs isolated from the CNS, draining lymph nodes (dLNs) and spleen of wild-type mice before ('naive',  $n = 3$ ), 12 days ('onset') or 17 days ('peak') after EAE induction ( $n = 4$  for CNS peak and spleen onset,  $n = 5$  otherwise). **e**, EAE in wild-type (WT) ( $n = 15$ ) and HIF-1 $\alpha$ <sup>Itgax</sup> ( $n = 9$ ) mice. Experiment repeated three times. **f**, IFN $\gamma$ <sup>+</sup>, IL-17<sup>+</sup> and IFN $\gamma$ <sup>+</sup>IL-17<sup>+</sup>GM-CSF<sup>+</sup> CD4<sup>+</sup> T cells in the CNS of wild-type and HIF-1 $\alpha$ <sup>Itgax</sup> mice 15 days after EAE induction ( $n = 5$

mice per group). **g**, RNA sequencing (RNA-seq) analysis of splenic DCs at peak EAE ( $n = 5$  mice per group). **h,i**, IPA (**h**) and GSEA for the human phenotype ontology term ‘abnormal activity of mitochondrial respiratory chain’ (**i**) in wild-type and HIF-1 $\alpha$ <sup>Htgax</sup> splenic DCs at peak EAE. NES, normalized enrichment score. **j**, Mean fluorescence intensity (MFI) of HIF-1 $\alpha$  expression in splenic DCs treated with metabolites and LPS for 6 h, normalized to LPS stimulation. DMF, dimethyl fumarate; Pyr, pyruvate; Mal, malonate; Succ, succinate; 4-OI, 4-octyl itaconate;  $\alpha$ -KG,  $\alpha$ -ketoglutarate; L-LA, L-sodium lactate ( $n = 4$  per condition). **k**, HIF-1 $\alpha$ <sup>+</sup> DCs after treatment with L-LA (0.1, 1 and 10 mM) and LPS for 6 h ( $n = 3$  for medium, L-LA 0.1 mM, L-LA 10 mM, LPS + L-LA 10 mM,  $n = 4$  otherwise). **l**, mRNA expression in wild-type BMDCs after treatment with LPS, L-LA, GPR81 antagonist or MCT1 inhibitor ( $n = 3$  per group). **m**, *Ifng*, *Il17a* and *Csf2* expression in 2D2<sup>+</sup>CD4<sup>+</sup> T cells co-cultured with wild-type BMDCs pre-stimulated with L-LA and LPS ( $n = 4$  for *Il17a* LPS + L-LA 0.1 mM,  $n = 3$  otherwise). **n**, *IFNG* and *IL17A* expression in human T cells co-cultured with DCs ( $n = 3$  per group). siNT, non-targeting siRNA. Statistical analysis was performed using one-way ANOVA with Dunnett’s or Šídák’s post-hoc test for selected multiple comparisons for **d,k,l–n**, unpaired Student’s *t*-test for **f** and two-way ANOVA for **e**. Data are mean  $\pm$  s.e.m.

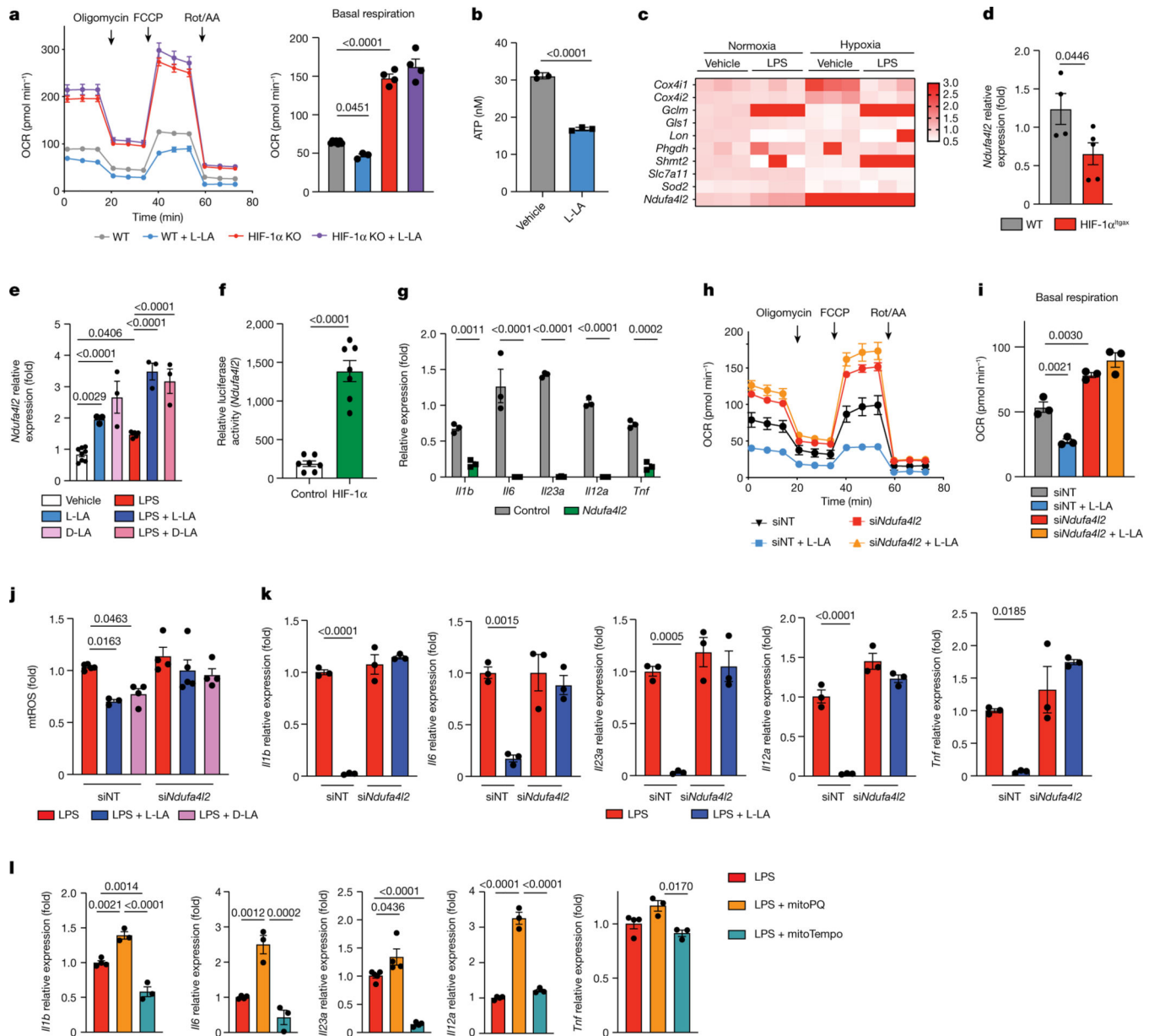


**Fig. 2 | HIF-1 $\alpha$ -induced NDUFA4L2 limits the production of mtROS.**

**a**, OCR in wild-type and HIF-1 $\alpha$ <sup>tgax</sup> BMDCs after stimulation with L-LA ( $n = 7$  for WT,  $n = 3$  for WT + L-LA,  $n = 4$  otherwise). **b**, ATP levels in BMDCs as a result of 1 mM L-LA for 6 h ( $n = 3$  per group). **c**, Expression of HIF-1 $\alpha$  target genes in BMDCs stimulated with LPS under normoxic or hypoxic conditions ( $n = 3$  per group). **d**, *Ndufa4i2* expression in wild-type and HIF-1 $\alpha$ <sup>tgax</sup> splenic DCs at EAE peak stimulation ( $n = 4$  for WT,  $n = 5$  for HIF-1 $\alpha$ <sup>tgax</sup>). **e**, *Ndufa4i2* expression after 6 h of treatment with LPS + L-LA, LPS + D-LA or LPS ( $n = 8$  for vehicle,  $n = 6$  for LPS,  $n = 3$  otherwise). **f**, Transactivation of the *Ndufa4i2* promoter after overexpression of HIF-1 $\alpha$  ( $n = 7$  per group). **g**, Effect of *Ndufa4i2* overexpression in LPS-stimulated BMDCs ( $n = 3$ ). **h–k**, Effect of *Ndufa4i2* knockdown on OCR (**h,i**), mtROS production (**j**) and gene expression (**k**) in BMDCs treated

with LPS, LPS + L-LA or LPS + D-LA ( $n = 3$  per group). **1**, mRNA expression in BMDCs treated with LPS, mitoPQ or mitoTempo for 6 h ( $n = 3$  per group). Statistical analysis was performed using one-way ANOVA with Tukey's, Dunnett's or Šídák's post-hoc test for selected multiple comparisons for **a,e,i-l**, two-way ANOVA for **g** and unpaired Student's  $t$ -test for **b,d,f**. Data are mean  $\pm$  s.e.m.

Author Manuscript

Author Manuscript

Author Manuscript

Author Manuscript

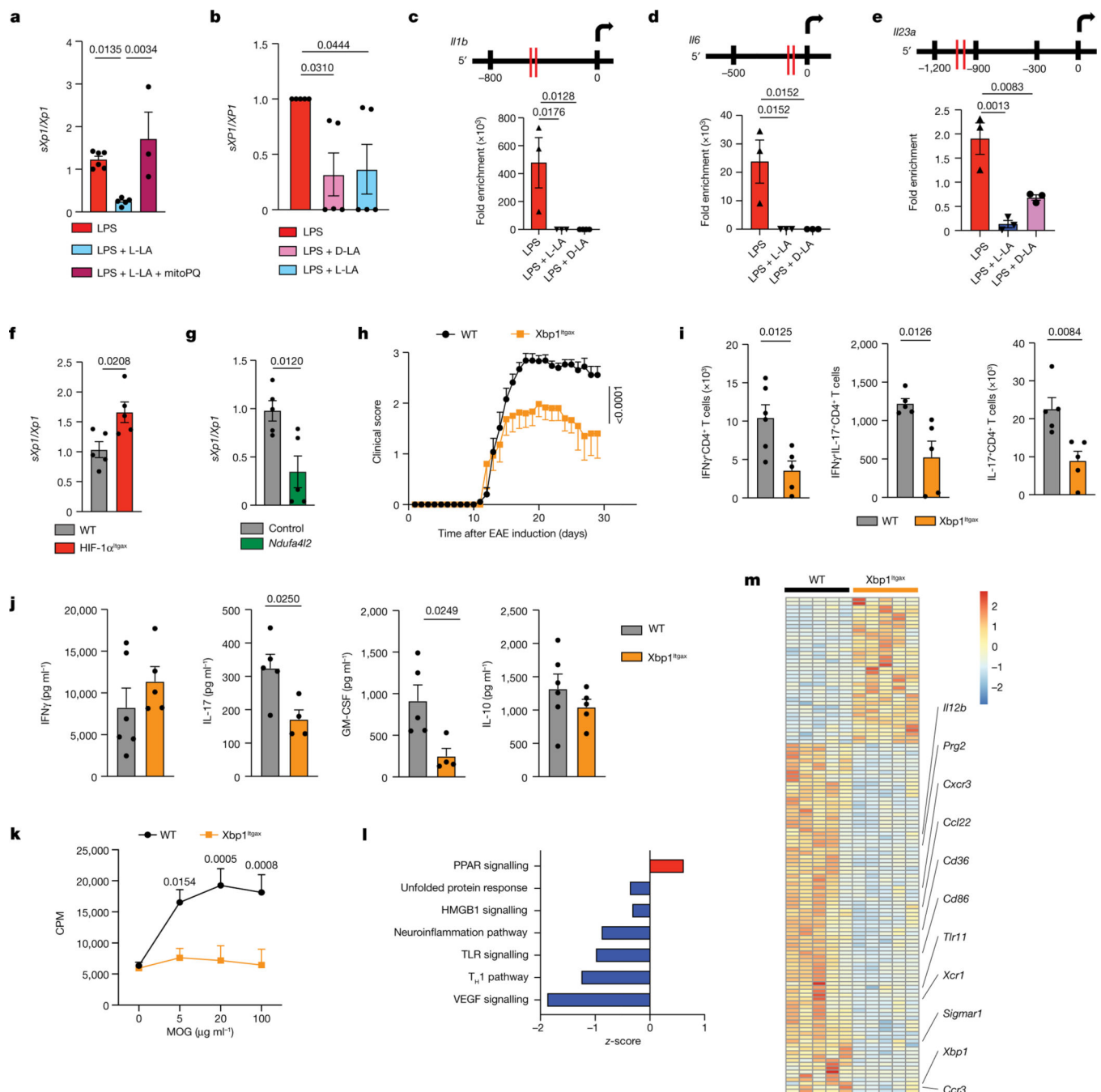


**Fig. 3 | L-LA limits the mtROS-driven activation of XBP1 in DCs.**

**a**, Spliced *Xbp1* mRNA normalized to total *Xbp1* mRNA ( $sXbp1/Xbp1$  ratio) in BMDCs isolated from wild-type mice and treated with LPS ( $n = 6$ ), LPS + L-LA ( $n = 5$ ) or LPS + L-LA + mitoPQ ( $n = 3$ ) for 6 h. **b**,  $sXPB1/XBP1$  mRNA ratio in human DCs treated with LPS, LPS + D-LA or LPS + L-LA for 6 h ( $n = 5$  per group). **c–e**, XBP1-binding sites (top) and recruitment of XBP1 to *Il1b* (**c**), *Il6* (**d**) and *Il23a* (**e**) promoters in BMDCs isolated from wild-type mice determined by chromatin immunoprecipitation (ChIP) after treatment with LPS, LPS + D-LA or LPS + L-LA for 6 h ( $n = 4$  for *Il1b* LPS + D-LA,  $n = 3$

otherwise). **f**, *sXbp1/Xbp1* mRNA ratio in wild-type ( $n = 5$ ) and HIF-1 $\alpha$ <sup>Itgax</sup> ( $n = 5$ ) splenic DCs isolated at peak EAE. **g**, *sXbp1/Xbp1* mRNA ratio in wild-type BMDCs transfected with either an empty plasmid ( $n = 5$ ) or an *Ndufa412*-overexpression plasmid ( $n = 5$ ). **h**, EAE development in wild-type ( $n = 15$ ) and XBP1<sup>Itgax</sup> ( $n = 15$ ) mice. Experiment repeated three times. **i**, IFN $\gamma$ <sup>+</sup>, IFN $\gamma$ <sup>+</sup>IL-17<sup>+</sup> and IL-17<sup>+</sup> CD4<sup>+</sup> T cells isolated from the CNS of wild-type ( $n = 5-6$ ) and XBP1<sup>Itgax</sup> ( $n = 5$ ) EAE mice. **j,k**, Cytokine production (**j**) and proliferative recall response to ex vivo MOG<sub>35-55</sub> restimulation for 72 h (**k**) of splenocytes from EAE wild-type and Xbp1<sup>Itgax</sup> mice ( $n = 6$  for IFN $\gamma$  and IL-10 WT,  $n = 5$  mice otherwise). CPM, counts per million. **l,m**, IPA (**l**) and heat map (**m**) of RNA-seq analysis of wild-type ( $n = 5$ ) and Xbp1<sup>Itgax</sup> ( $n = 5$ ) splenic DCs isolated 30 days after EAE induction. Statistical analysis was performed using one-way ANOVA with Dunnett's or Šídák's post-hoc test for selected multiple comparisons for **a-e**, unpaired Student's *t*-test for **f,g,i,j** and two-way ANOVA for **h,k**. Data are mean  $\pm$  s.e.m.

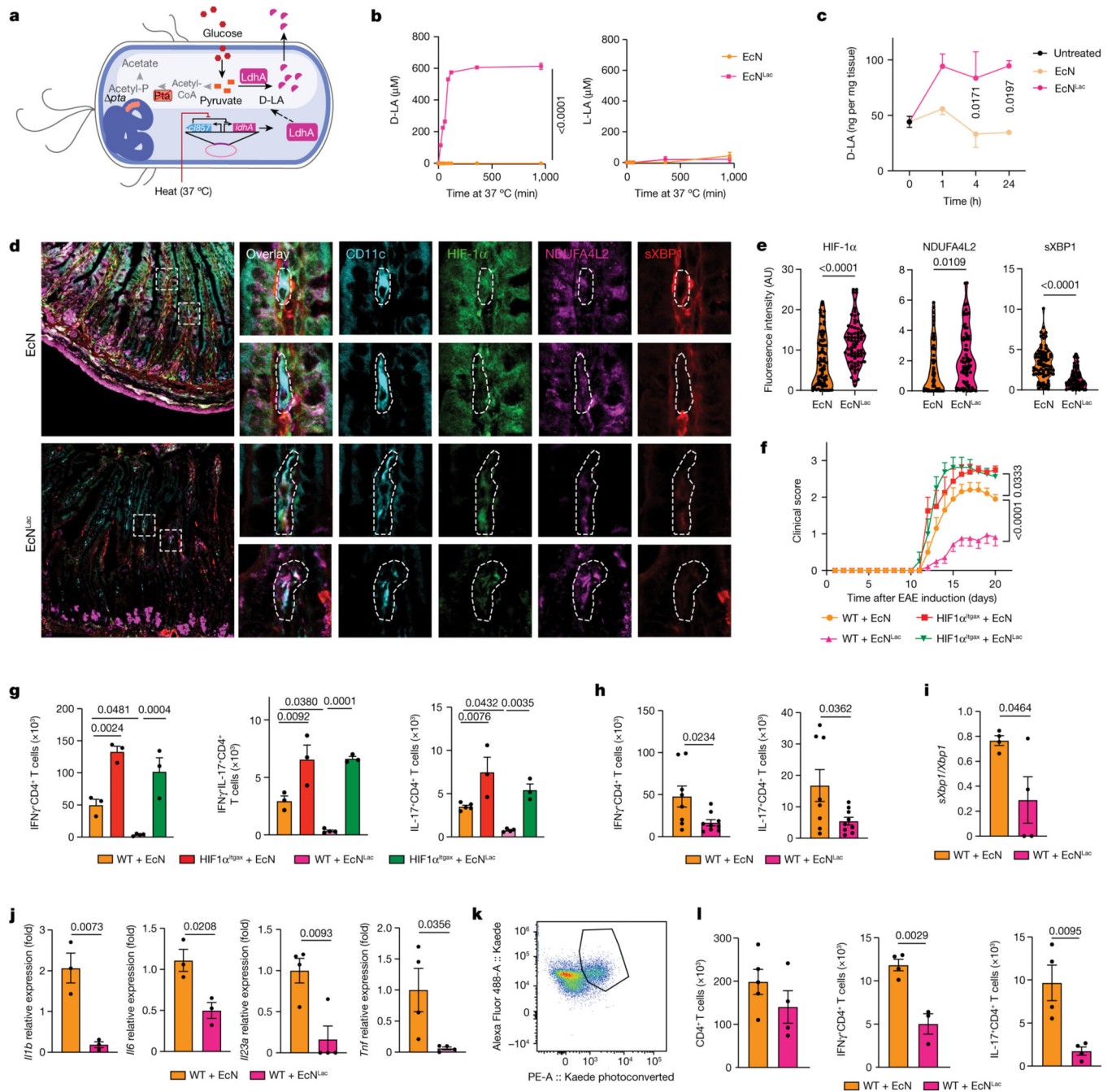


**Fig. 4 | Activating HIF-1 $\alpha$ -NDUFA4L2 with engineered probiotics ameliorates EAE.**

**a**, Engineered EcN<sup>Lac</sup> strain. **b**, Concentrations of D-LA and L-LA in culture supernatants after EcN<sup>Lac</sup> or EcN incubation at 37 °C ( $n = 3$  per group). **c**, Concentration of D-LA in small-intestinal tissue after daily administration of EcN ( $n = 3$  at 1 h and 24 h,  $n = 5$  at 4 h) or EcN<sup>Lac</sup> ( $n = 4$  at 1 h and 24 h,  $n = 5$  at 4 h) for a week compared to untreated controls ( $n = 5$  mice). **d,e**, Immunostaining analysis of HIF-1 $\alpha$ , NDUFA4L2 and spliced XBP1 (**d**) and quantification (**e**) in CD11c<sup>+</sup> cells from the small intestine after daily administration of EcN<sup>Lac</sup> or EcN for a week ( $n = 5$  mice per group). Data quantified from tile scan images

of full tissue sections from each mouse. Experiment repeated twice. AU, arbitrary units. **f**, EAE in wild-type and HIF-1 $\alpha$ <sup>Itgax</sup> mice treated with EcN ( $n = 5$  WT, 5 HIF-1 $\alpha$ <sup>Itgax</sup> mice) or EcN<sup>Lac</sup> ( $n = 19$  WT, 4 HIF-1 $\alpha$ <sup>Itgax</sup> mice). Experiment repeated three times. **g**, Quantification of IFN $\gamma$ <sup>+</sup>, IL-17<sup>+</sup> and IFN $\gamma$ <sup>+</sup>IL-17<sup>+</sup> CD4<sup>+</sup> T cells in the CNS of mice from **f** ( $n = 5$  for IL-17 WT EcN,  $n = 4$  for WT EcN<sup>Lac</sup>,  $n = 3$  otherwise). **h**, Quantification of IFN $\gamma$ <sup>+</sup> and IL-17<sup>+</sup> CD4<sup>+</sup> T cells in the small intestine of wild-type mice treated with EcN ( $n = 8$ ) or EcN<sup>Lac</sup> ( $n = 9$ ) after EAE induction. **i,j**, *sXbp1/Xbp1* mRNA ratio (**i**) and *Iilb*, *Il6*, *Il23a* and *Tnf* mRNA expression (**j**) in small-intestinal DCs from EcN- or EcN<sup>Lac</sup>-treated mice ( $n = 4$  for *Il23a* and *Tnf*,  $n = 3$  otherwise). **k**, Representative dot plot of Kaede photoconversion in CD4<sup>+</sup> T cells isolated from the spleen. **l**, Total, IFN $\gamma$ <sup>+</sup> and IL-17<sup>+</sup> CD4<sup>+</sup> T cells photoconverted in the spleen of wild-type mice treated with EcN ( $n = 5$ ) or EcN<sup>Lac</sup> ( $n = 4$ ). Statistical analysis was performed using two-way ANOVA followed by Šídák's multiple comparisons test for **b,c,f**, unpaired Student's *t*-test for **e,h-j,l** and one-way ANOVA with Šídák's post-hoc test for selected multiple comparisons for **g**. Data are mean  $\pm$  s.e.m.

**Table 1 |**

Genes associated with the response to mitochondrial depolarization (GSEA GO:0098780)

<b>Symbol</b>
<i>Ambra1</i>
<i>Atg13</i>
<i>Atg14</i>
<i>Atp5if1</i>
<i>Becn1</i>
<i>Cdc37</i>
<i>Gba1</i>
<i>Gps2</i>
<i>Hdac6</i>
<i>Hk2</i>
<i>Htra2</i>
<i>Huwe1</i>

Author Manuscript

Author Manuscript

Author Manuscript

Author Manuscript